Analysis and Design of Single-Fed Circularly Polarized Circular Microstrip Antennas

A. E. Abdulhadi

A Thesis

in

The Department

Of

Electrical and Computer Engineering

Presented in Partial Fulfillment of the Requirements

For the Degree of Master of Applied Science (Electrical Engineering) at

Concordia University, Quebec, Canada

March 2007

Your file Votre référence
ISBN: 978-0-494-28907-5
Our file Notre référence
ISBN: 978-0-494-28907-5

Abstract

Analysis and Design of Single-Fed Circularly Polarized Circular Microstrip Antennas

A. E. Abdulhadi

A novel design of a circular microstrip antenna with an additional small circular patch excited by a single feed for achieving a dual band frequency operation with circular polarization (CP) is presented. The implemented dual band circularly polarized antenna has a compact configuration that serves the technology demands requirements in mobile unit systems for smaller volume. Simulation and experimental results show that the 10 dB return-loss impedance bandwidth is better than that of a conventional single circular microstrip patch antenna. In addition, a dual frequency band operation at 2.45 GHZ and 5.2GHZ is obtained.

A second antenna design suitable for an integrated circuits demand is also presented. Results demonstrate that both sense left hand and right hand circular polarization (RHCP, LHCP) can be achieved using this technique. A comparison between theoretical and experimental results is provided and shows good match. The resonance frequencies and quality of the axial ratio can be controlled by changing the radii of the two circles, and the orientation of the additional circular patch relative to the main patch.

For other desired frequencies, the design of the antenna can be carried out by calculating the radii of the main and additional patch using empirical equations acquired for this design. The empirical formulas are developed based on a comprehensive parametric study where different designs and material parameters are varied to achieve an optimum antenna performance.

A 64-element uniform linear array of circular microstrip patch antennas is designed and simulated for achieving circular polarization (CP) with more than (20 dB) directivity. Since the axial ratio bandwidth of the implemented antenna is narrow, a sequential rotation of radiating patches with suitable excitation phase shifting has been applied to improve the polarization purity over a wide range of frequencies with higher gain compared to a single patch.

Acknowledgements

I would like to thank my advisor Dr. A. Sebak for the time he spent with me, not only for the thesis, but also for the antenna course which was given by him. I would also like to thank Libyan education program for funding me to pursue my education in Canada. I would like to thank my friend Wadah for his encouragement and his friendship. I would like to thank INRS research center in Montréal for the pattern measurements.

Finally I would like to thank my family, specially my parents for their support and their prayers to be a successful student. I would also like to express my gratitude to my wife for her support.

TABLE OF CONTENTS

LIST OF FIGURES

Figure

ABBREVIATIONS

MPA	Microstrip Patch Antenna
CP	Circular Polarization
LHCP	Left Hand Circular Polarization
RHCP	Right Hand Circular Polarization
LP	Linear Polarization
ISM	Industrial, Scientific, and Medical Band
CPMPA	Circularly Polarized Microstrip Patch Antenna
GPS	Global Position System
GTD	Geometrical Theory of Diffraction
SCPMA	Single-feed-type Circular Polarized Microstrip Antenna
SAR	Synthetic Aperture Radar
IE	Integral Equation
PDE	Partial Differential Equation
PTD	Physical Theory of Diffraction
MOM	Method of Moment
EFIE	Electrical Field Integral Equation
AR	Axial Ratio
BW	Bandwidth

LIST OF SYMBOLS

TM_{11}	Dominant resonance mode
Q	Quality factor of patch antenna
Q_D	Dielectric factor of patch antenna
Q_R	Radiation factor of patch antenna
Q_C	Conductor factor of patch antenna
$f_r(GHz)$	Resonant frequency
Δf	Bandwidth between the $3dB$ return losses
$c\left(m.s^{-1}\right)$	Speed of light
$h(mm)$	Thickness of the substrate
$k\left(m^{-1}\right)$	Wave number
$Z_T(\Omega)$	Impedance of the transmission line
$E^e\left(V.m^{-1}\right)$	Electrical excitation fields
$E^d\left(V.m^{-1}\right)$	Electrical diffracted fields
$\mathbf{J_s}\left(A.m^{-1}\right)$	Surface current density
$\overline{\mathbf{G}}_A\left(\Omega.s.m^{-2}\right)$	Dyadic Green's functions for the vector potential
$\overline{G}_V\left(F^{-1}\right)$	Dyadic Green's functions for the scalar potential
$L(f)$	Linear operator
ε_r	Relative permittivity
α_{nm}	*mth* zero of the derivative of the Bessel function of order *n*
ε_{eff}	Effective relative permittivity
S_{11}	Return losses
$HPBW(\text{degree})$	Half power beam width
$R_1(mm)$	Radius of the main circular patch
$R_2(mm)$	Radius of the additional circular patch
D	Directivity
G	Gain
$P_r(w)$	Radiated power
e_r	Radiation efficiency

Chapter One

Introduction

1.1 Motivation

With the surge in today's mobile communication systems, the requirements to build low-cost, lightweight, and low-profile mobile units have accordingly increased. Recently, microstrip patch antennas have been studied extensively because their advantages can satisfy these requirements.

A conventional microstrip antenna in general consists of a conducting patch on a grounded microwave substrate. Microstrip antennas have attractive advantages of low cost, light weight, easy fabrication, and simplicity to mounting hosts. In spite of limitations such as small bandwidth, low gain and power handling capability, microstrip antennas offer some advantages over other types of antennas due to their increasing use in a variety of applications such as an industrial, scientific, and medical band (ISM) wireless communication, and military applications. Increasing demands for circularly polarized microstrip antennas $(CPMPA's)$ and a dual band operation for communication systems have aimed on improving the performance of microstrip antennas.

Various types of circularly polarized microstrip antennas have been studied with various feeding techniques. Based on the number of feeding points, circularly polarized microstrip antennas can be classified as a single- or dual-feed. A dual feed is used with 90^0 phase shift between the feeding. Dual-fed circularly polarized patches require an

additional circuit, which adds more complexity for antenna array designs. A single-fed antenna is used to generate CP with a special perturbation in the patch such as a patch with slots, a truncated corner square patch, and a truncated tip triangle patch. Although, dual feed circularly polarized antennas have wider axial ratio bandwidth than single feed antennas, single feed circularly polarized antennas received much attention. Single feed circularly polarized antennas allow reduction in the complexity of the feeding network, weight, and are more compact using less board space than dual feed CP techniques. In addition, the single-fed circularly polarized patches are very attractive because they can be arrayed and easily fed like any linearly polarized patches.

Since single feed circularly polarized antennas have a narrow axial ratio bandwidth. A sequential rotated array is used to improve the axial ratio bandwidth of antennas. This technique is suitable with microstrip patch antennas; because the phase between the elements can be designed with appreciate lengths of network feeding.

1.2 Objective

The objective of this research is to investigate and develop a simple design procedure that would allow the design of simple single feed low profile circularly polarized circular microstrip patch antennas. The antenna would match the state of the art microstrip patch antennas $(MPA's)$ devices presently on hand for feasible uses in industrial, scientific, and medical band (ISM) wireless communication applications. Instead of using slots or using two feeding in a microstrip antenna to achieve circular polarization, the main objective of this research is to introduce a new design that uses an additional patch to create circular polarization.

The thesis undertaken will focused on the performance and characterization of a circularly polarized microstrip antenna with single feed, and investigate its properties such as far field radiation pattern, polarization, bandwidth, and directivity.

The aim of the design is to design three antennas. One is a dual band circular polarized microstrip patch antenna, and it covers both bands (2.45 GHz, 5.2 GHz) ISM band. The second type is a circularly polarized microstrip antenna integrated with a microstrip transmission line to meet the demands of integrated circuits. Also, the uniform linear array circularly polarized antenna for achieving 20 dB directivity is designed at the same band 2.45 GHz. The third design is made at 5.2 GHz with around 10%, 10 dB return loss bandwidth. Both types of circularly polarized (RHCP, LHCP) antennas are designed. A 2×2 of sequentially rotating antenna patches in an array environment are applied for a wide bandwidth axial ratio.

1.1 Organization

This thesis is presented in a number of chapters. Chapter one presents a general overview of the thesis, its approach, introduction, and objective.

Chapter two contains a review of circularly polarized microstrip antennas. It continues with a general discussion on microstrip patch antennas. Next, a rapid review of some work done to date on circularly polarized microstrip antennas (CPMPA's) is presented. The major design characteristics are presented including the advantage and disadvantage of this technology. In addition, a brief background of dual frequency techniques of MPA's is given. Also, it provides a brief discussion of a full wave technique that is used to analyze microstrip antennas, which includes the definition, and advantages of full wave analysis. This chapter discusses a simulation technique that is

used in this work. The numerical technique, method of moment (MOM) has been briefly discussed in this chapter.

Chapter three introduces a novel design of a circular microstrip antenna with an additional patch excited by a single feed (Coaxial cable) for achieving a dual band frequency operation with circular polarization (CP). Also, introducing a circularly polarized antenna fed by a transmission line microstrip to serve demands of an integrated circuit. A description of the design approaches and geometries of the fabricate antennas are also given. Also, it introduces the practical aspects of the research undertaken

Chapter four introduces a microstrip antenna array with circular polarization that is designed to meet demands of base satiation antennas, personal communications, and global position systems (GSP). To improve the axial ratio of a single feed antenna, the sequential rotated feeding technique is used. The phase rotated technique used in this thesis is $0^0, 90^0, 180^0, 270^0$ rotation. A comparison between simulated and measured results is given in this chapter.

Finally, chapter five presents the conclusion of the research based on the experimental and theoretical work. It also introduces some topics for future work.

C h a p t e r T w o

Literature Review

2.1 Overview

This chapter provides a review of circularly polarized microstrip antennas. It continues with a general discussion of a microstrip patch antenna. Next, a general review of the research and development of circularly polarized microstrip antennas (CPMPA) technology is given. The review begins with dual feed circularly polarized microstrip antennas (CPMPAs), and then quickly focuses on methods for producing single feed circularly polarized antennas. In addition, a brief back ground of dual frequency techniques of (MPA's) is presented. Also, it provides a brief discussion of a full wave technique used to analyze microstrip antennas including the definition, and advantages of full wave analysis. The numerical technique based on method of moment is briefly discussed in this chapter.

2.2 Microstrip Antenna

2.2.1 Introduction

In 1952 Grieg and Engleman [1], gave first introduction to realization of radiators which are compatible with microstrip transmission lines. However, the concepts of microstrip geometries which radiate electromagnetic waves as an antenna were proposed by Deschamaps in 1953 [1] [2]. In 1955 a patent of a microstrip antenna design was awarded to Gutton and Baissinot [2]. The first practical antenna was built by Howell and

munson [3] [1]. Because of its numerous advantages such as: light weight, low volume, low cost, conformal configurations, extensive researches have been done to develop microstrip antennas.

2.2.2 Definition of a Microstrip Antenna

The simplest microstrip antenna geometry consists of a radiating patch which is usually made from a very metallic strip. The common metallic strip is copper, and in some designs is from gold. The shapes of a patch conductor can be designed to be any shape, but the common shapes are square, rectangular, or circular patches. They are common because of ease of analysis and fabrication [1]. The patch antennas are printed on the upper side of dielectric substrates as shown in figure 2.4. The lower side of dielectric substrates is a ground plane. The patch is fed by a microstrip transmission line or a coaxial cable. Microstrip transmission lines are printed on the upper side. Coaxial cable feeding is connected to the patch antenna through the ground. Array of microstrip elements with single or multiple feeds may also be used to produce more directivity.

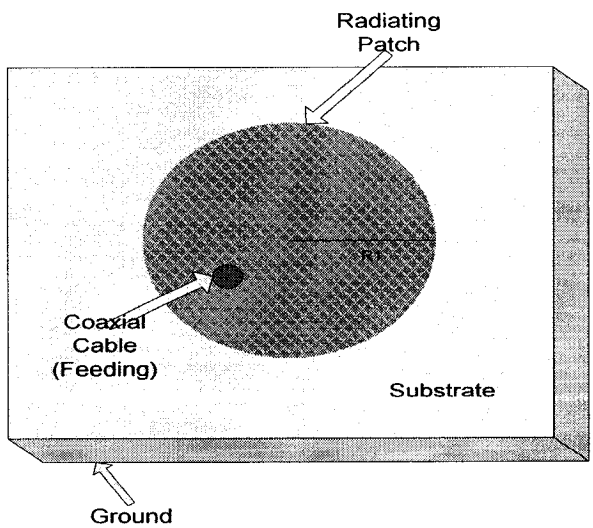

Figure 2.1: Microstrip antenna configuration

2.2.3 Types of Microstrip Antenna Configuration

Microstrip antennas may be made of any geometrical shape and any dimension. However, all microstrip patch antennas can be divided into three basic categories: microstrip patch antennas, microstrip traveling wave antennas and microstrip slot antennas [1].

2.3 Antenna Polarization

The core factors required to estimate an antenna's performance include radiation pattern, gain, impedance bandwidth and polarization. Antenna polarization is a very imperative consideration when selecting and establishing an antenna. Knowing the difference between polarizations and how to take advantage of their benefit is very significant to the antenna applications.

2.3.1 Circularly Polarized Microstrip Antennas and Techniques

In general microstrip patch antennas are linearly polarized, but they could be designed to generate circular polarization using some techniques. In general circular polarization techniques are depending on the number of feeding or the shape of the patch antenna. In this thesis, our discussion will be focus on resonator patch antennas. Every technique has advantages and disadvantages in terms of the axial ratio bandwidth, and the complexity of the antenna design procedure or antenna fabrication.

2.3.2 Circularly Polarized Patch Antenna Techniques

Recently, various types of circularly polarized microstrip antennas (CPMA'S) have been studied with various feeding techniques. There are two commonly used circularly polarized microstrip antennas [4]: single feed and dual feed patch antennas. Although the axial ratio of single feed circularly polarized antennas is narrow, they are very attractive because they can be arrayed and easily fed like any linearly polarized antennas [5]. Dual feed circularly polarized antennas require an additional circuit that requires more space and adds more complexity for array designs.

2.3.3 Dual-Orthogonal Feed Circularly Polarized Microstrip Antennas

Two feeds can be located on the printed antenna in such way that two linearly polarized waves with perpendicular polarization planes are produced. This technique produces a dual polarized antenna that can transmit, and receive independently two orthogonal linearly polarized waves. When two feeds are fed by signals that have equal amplitude, and 90^0 phase shift the antenna can be used to transmit or receive circular polarization [6].

2.3.4 Dual-Feed Structures

Dual linear polarization can be obtained using a patch with a symmetrical shape, which is most often a square or a circular patch. A structure with double feeds for generating two polarized waves is shown in figure 2.2. Also, figure 2.3 presents a transmission line feed that is printed on the same substrate of the patch antenna.

This technique is a direct way to generate circular polarization. However, there are disadvantages using this type of technique such as more space requirements, complexity to feed the antenna array, complexity to match with RF devices: amplifier, mixer, low noise amplifier...etc.

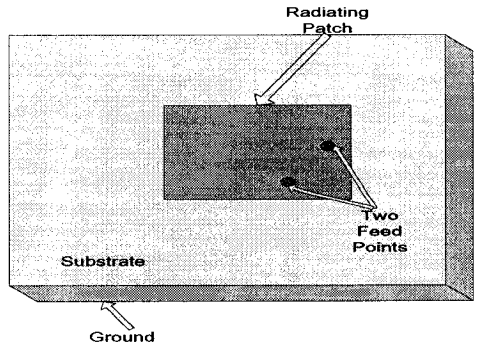

Figure 2.2: Excitation of dual linear polarization by coaxial cables

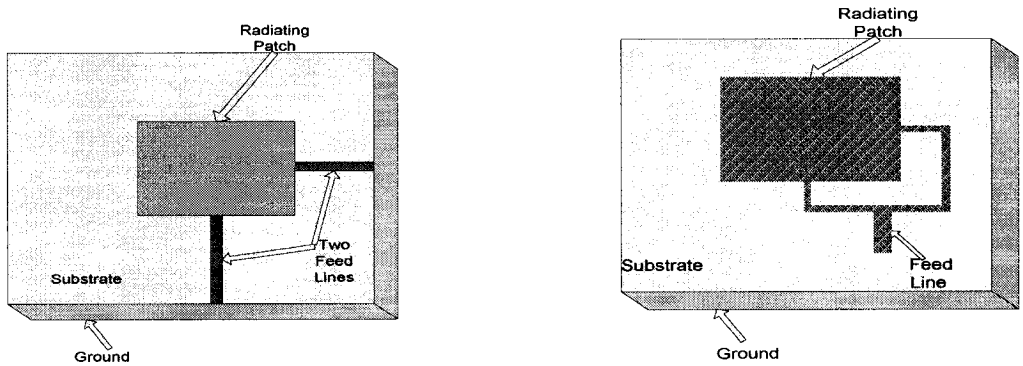

Figure 2.3: Excitation of dual linear polarization by transmission lines

2.3.5 Examples of Using Two Feed, Four Feed Coaxial Cables

Circular microstrip patch antennas at higher modes with circular polarization have been studied in [7]. For circular polarization, two feeds with appropriate angular spacing are required as shown in Figure 2.4. The fields that generated from the two feeds are

orthogonal to each other inside the patch as well as outside the patch, when the required spacing is implemented. To generate circular polarization, the two probes are required to be fed 90^0 out of phase, and equal amplitude.

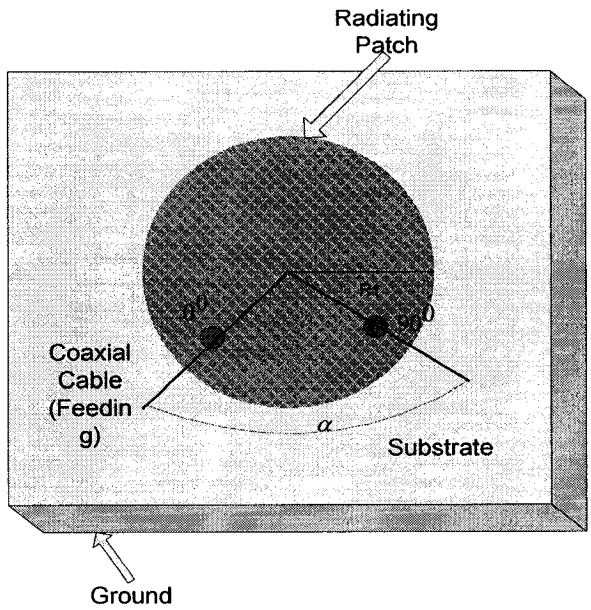

Figure 2.4: Two-probe feeds with proper angular spacing for exciting circular polarization

Angular spacings are tabulated in Table (2.1), where the angular spacing between two feed probes is different for each different mode [7].

	TM_{11}	TM_{21}	TM_{31}	TM_{41}	TM_{51}	TM_{61}
α	90^0	45^0 or 135^0	30^0 or 90^0	22.5^0 or 67.5^0	18^0,54^0 or 90^0	15^0,45^0 or 75^0

Table 2.1: Feed probe angular spacing for circular polarization at different resonance modes [7]

In order to maintain a symmetry beam and to keep low cross polarization, especially for quite thick substrate radiators, the unwanted modes need to be suppressed. Adding two additional feed probes located diametrically across from the two original feeds will minimize the unwanted modes [7]. The required angular spacing for these four feeds should have a phase arrangement of space 0^0,90^0, 0^0,90^0 for the even order modes, and 0^0,90^0,180^0,270^0 for the odd-order modes. Using this technique, the fields of the unwanted modes from the two opposing feeds cancel. Figure 2.5 presents the feed angular and phase arrangements for different modes.

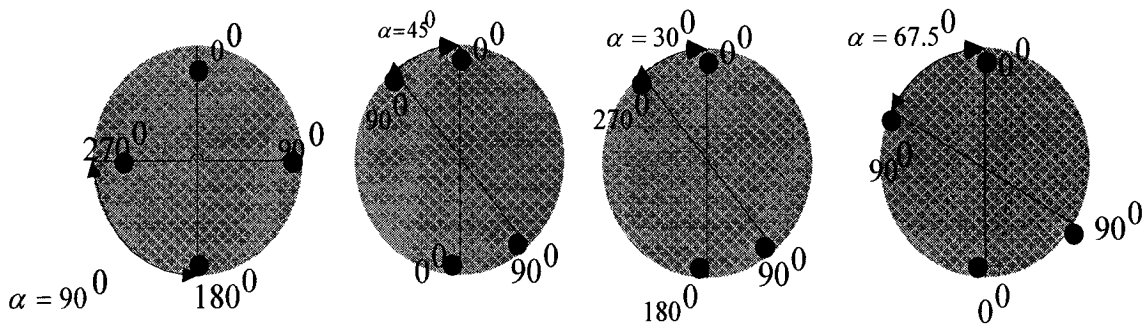

Figure 2.5: Four-probe feeds with proper angular and phase arrangements for exciting different resonant modes with circular polarization

A microstrip antenna with higher mode excitation can be efficiently used as a conformal land mobile antenna or as an aircraft antenna for satellite communication. Higher order mode elements can also be used for low angle scanning applications.

Figure 2.6 demonstrate that the peak of the conical pattern can be scanned over a wide angular range from 38^0 to about 60^0 from the circular patch broadside.

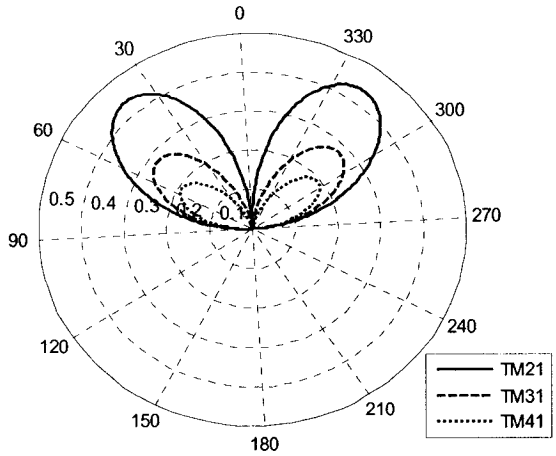

Mode	Dielectric constant	Peak direction from zenith	Radius of the patch
TM_{21}	2.2	$\approx 38^0$	0.0401m
TM_{31}	2.2	$\approx 45^0$	0.0552m
TM_{41}	2.2	$\approx 60^0$	0.0698m

Figure 2.6: Computed radiation patterns in an elevation plane for $TM_{21}, TM_{31}, TM_{41}$ modes at 2.45GHz

Clearly, the radiation pattern of the antenna is similar to a monopole antenna. Co-Polarization and Cross-Polarization for a circularly polarized circular microstrip antenna at higher modes are studied in [8].

2.4 Single-Feed Circularly Polarized Microstrip Antennas

Single feed circularly polarized microstrip antennas have many advantages compared with dual-fed antennas. Single feed circularly polarized microstrip antennas are more compact than that used for dual feeds. They can be printed on small size boards. The commonly known circularly polarized microstrip antennas are a square or a circular patch, and many of them are presented with detail in [9]. Other CP designs with a compact patch size are reported later in this thesis.

2.5 Previous Designs (Single-Feed Circularly Polarized Microstrip Antennas)

The concept of generating circular polarization (CP) using microstrip antennas with single-feed is based on generating two orthogonal modes with the same amplitude and 90^0 phase different.

2.5.1 The TM_{11} Quadrapolar Mode

Single feed circularly polarized microstrip antennas can be designed using a circular patch excited with TM_{11} mode [10]. Circular polarization can be generated by stretching a circular patch into an ellipse patch, and feeding the antenna at $\phi = \pm 45^0$. Then a pair of orthogonal modes will be generated. The ratio of the semi-major to semi-minor axes which will produce circular polarization is given by [10]:

$$\frac{a}{b} = 1 + \frac{1.0887}{Q} \tag{2.1}$$

The value of Q can be computed using the cavity model equation in Appendix A (A.21) and it is given by:

$$\frac{1}{Q} = \frac{1}{Q_R} + \frac{1}{Q_D} + \frac{1}{Q_C} \tag{2.2}$$

Where

Q_D is the dielectric quality factor and it is given by:

$$Q_D = \frac{1}{\tan\sigma} \tag{2.3}$$

Q_R is the radiation Q and it is given by:

$$Q_R = \frac{240\left[(Ka)^2 - n^2\right]}{h\mu f_r (k_o a)^2 I_1} \tag{2.4}$$

Q_C is the conductor Q and it is given by:

$$Q_C = h\sqrt{\mu_0 \pi f_r \sigma_c} \tag{2.5}$$

h is the thickness of the substrate, and k is the wave number.

Also, it is possible to find Q by estimation:

$$Q \approx \frac{f_o}{\Delta f} \tag{2.6}$$

Where

f_0 is the resonant frequency, and Δf is the bandwidth between the $3dB$ return losses points

If the radius of the unperturbed circular patch which operates at a desired design

frequency f_o is designated as a', the semi-major axis a and semi-minor b of the ellipse which produces circular polarization may be written as:

$$a = a' + \Delta L \tag{2.7}$$

$$b = a' - \Delta L \tag{2.8}$$

Where

$$\Delta L = \frac{a'}{\left(\frac{2Q}{1.0887}\right)+1} \tag{2.9}$$

Figure 2.7 shows the shape of the antenna perturbed into an ellipse to generate circular polarization.

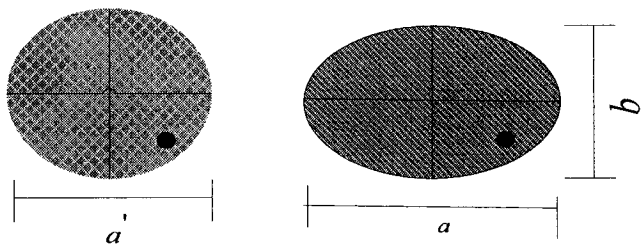

Figure 2.7: Shape of an antenna perturbed into an ellipse to generate circular polarization

2.5.2 Using Perturbation Segments

The single-feed-type circularly polarized microstrip antenna (SCPMA) with a perturbation segment ΔS as shown in figure 2.8.b, 2.8.c have been rapidly presented in

recent years, because they permit circular polarization without using additional feeding. Circular polarization achieves by adjusting the perturbation segment ΔS to produce orthogonal modes with equal amplitude, and in the quadrate phase. This design is presented in detail [11].

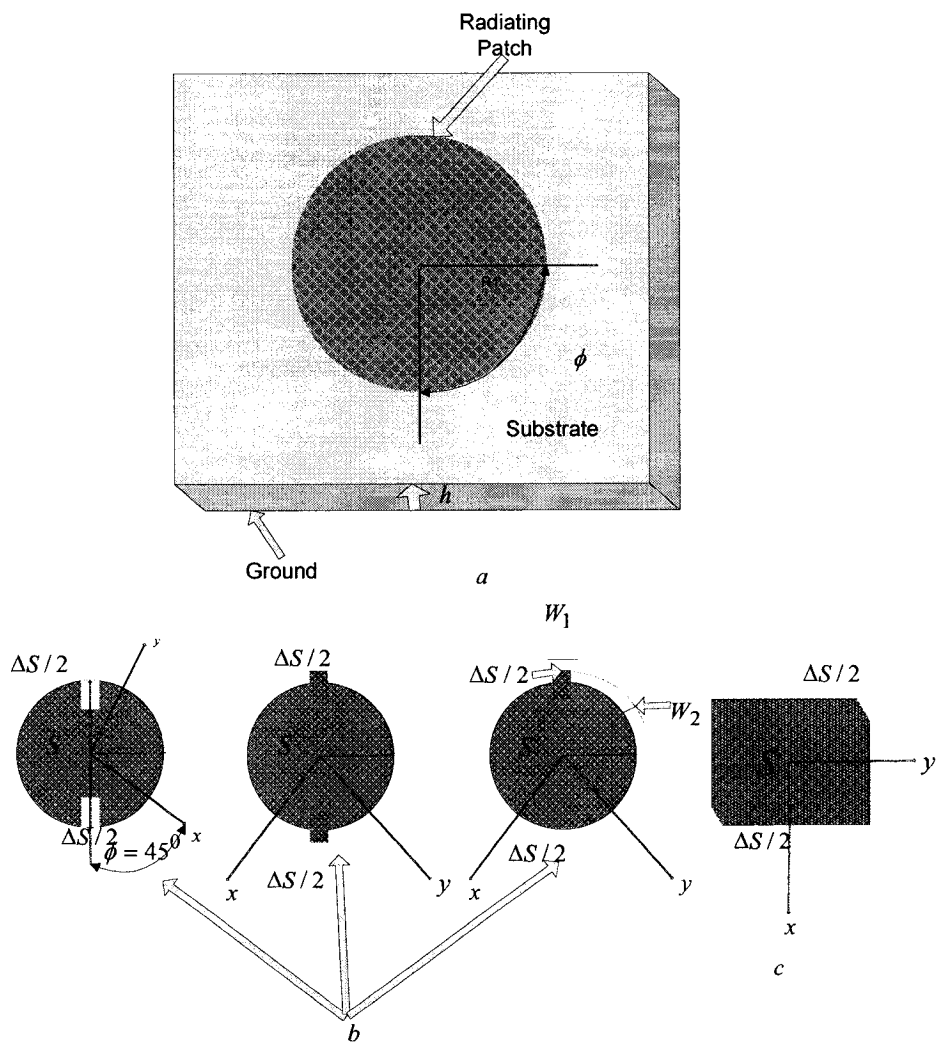

Figure 2.8: Configuration of a single-feed-type circularly polarized microstrip antenna

2.5.3 Using a Slit or a Pair of Slits

2.5.3.1 Design with a Slit for a Circular Patch

CP radiation of a microstrip antenna can be achieved by designing the antenna with a single slit that is inserted to the boundary of a microstrip patch and feeding the antenna with a single feed along an axis 45^0 to the plane that has a slit, Applications of this CP design technique to square and circular microstrip patch antennas in detail in [12]. Figure 2.16 shows the geometry of a circular microstrip patch antenna with a slit for CP radiation. The length of the slit is l, the width is w, and $(l \rangle\rangle w)$. The feed at point C along the diameter AB is for RHCP radiation, while point D is for LHCP operation. Also, this technique has been successfully applied to triangular and rectangular microstrip patch antennas in [14] [15] [16].

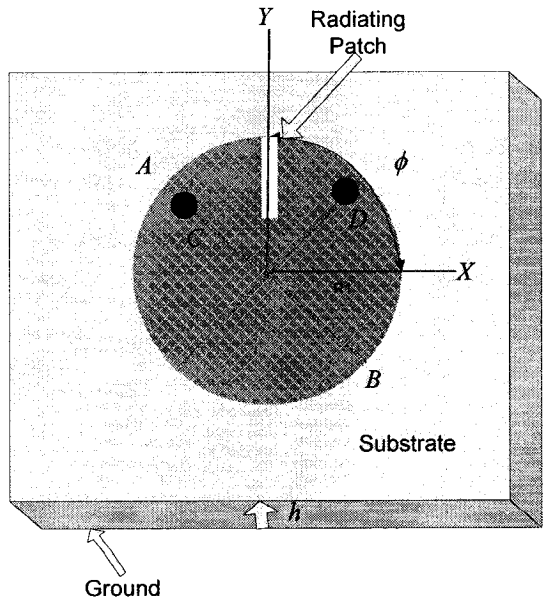

Figure 2.9: Geometry of a microstrip antenna with a slit for CP radiation, feed at point *C* is for RHCP operation, and point *D* is for LHCP operation

2.5.3.2 *Design with Four Slits for a Circular patch*

This technique is used four slits for generate CP radiation. Narrow slits of length $l/2$ and width 1mm is located at the border line of the circular patch. Each pair of slits has equal width and same length for the same plane [17]. Lengths of two pairs of slits l_x, and l_y are unequal, but they have the same width as shown in Figure 2.10.

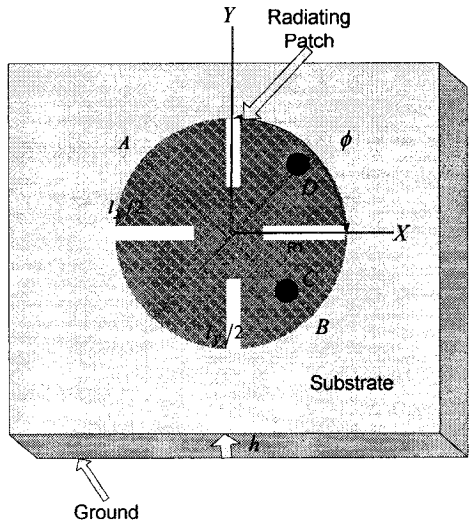

Figure 2.10: Geometry of a circular microstrip antenna with slits for CP radiation Feed at point C is for RHCP and point D is for LHCP

2.5.3.3 *Design with a Pair of Slits*

CP operation can be obtained using an annular-ring microstrip patch antenna. A pair of slits is inserted at its inner boundary to produce CP radiation. Two examples of the antenna fed using a microstrip transmission line at the inner and outer patch boundaries have been studied in [18]. For RHCP operation, the microstrip feed line will

be located at the $(\phi = 45^0)$ plane, and for LHCP operation microstrip feed line will be located at the $(\phi = 135^0)$ plane as shown in figure 2.11. The transmission line section that transforms impedance between a 50Ω microstrip line and the outer/inner patch boundary is calculated by equation (2.10) instead of quarter wave transform for good matching [18].

$$50 = Z_T[(Z_A + jZ_l \tan \beta l)/(Z_T + jZ_A \tan \beta l)] \qquad (2.10)$$

Where, Z_A is the impedance at the outer/inner of patch boundary, Z_T is the characteristic impedance of the transmission line section, and β is the wave number.

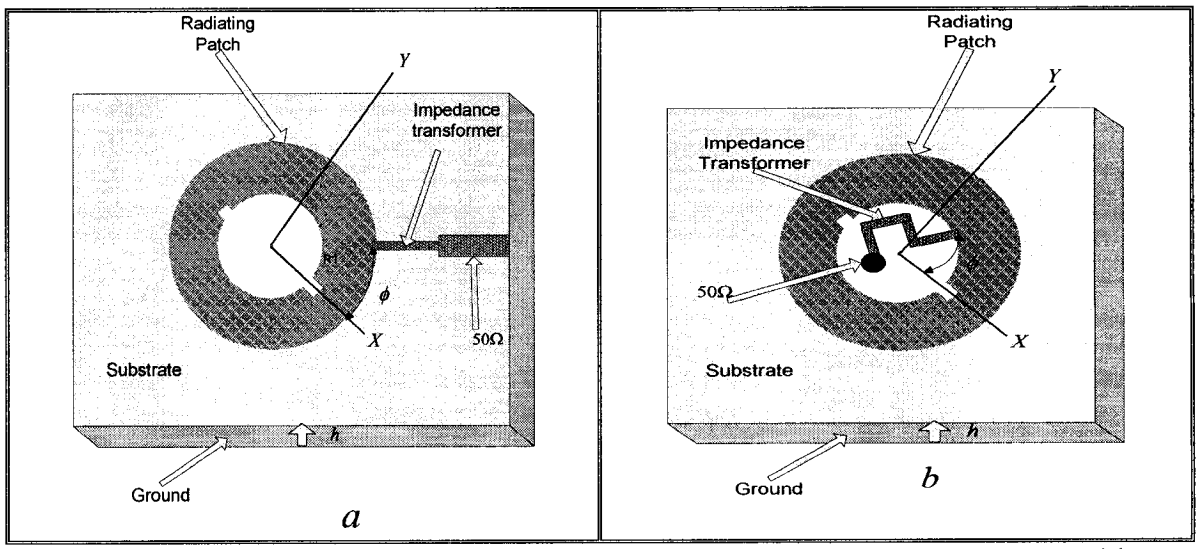

Figure 2.11: Geometry of a circularly polarized annular-ring microstrip antenna with a pair of inserted slits. a) Microstrip feed line at the outer boundary of the patch. b) Microstrip feed line at the inner boundary of the patch

2.5.4 Designs with a Tuning Stub

2.5.4.1 Circular Patch Antenna

Figure 2.12 shows a circularly polarized microstrip patch antenna design with a tuning stub. Inserted a tuning stub of length l_s and width 1 mm at the patch boundary in the x direction or $\hat{y}$ direction, will generate a slightly lower resonant frequency depending on the location of the slit. By choosing the suitable stub length and exciting the patch at a point A LHCP radiation will be generated, and at point RHCP radiation will be generated [19].

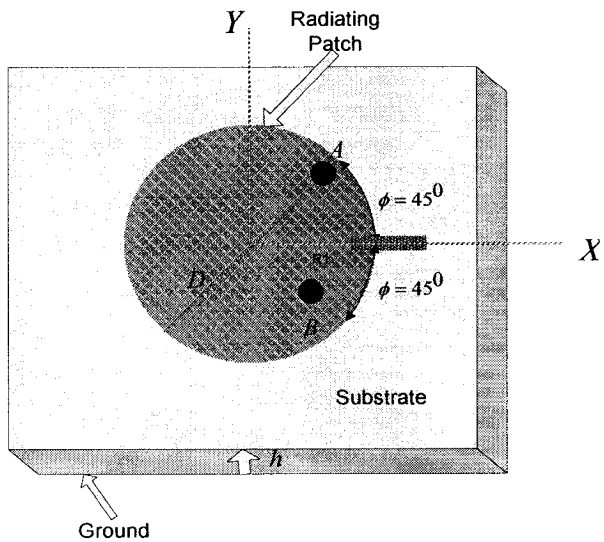

Figure 2.12: Geometry of a circularly polarized circular microstrip patch antenna with a tuning stub

2.5.4.2 Circular Patch Antenna with a Cross slot

A tuning stub technique has been applied to a circular microstrip patch with a cross slit of equal slot lengths. The antenna geometry is shown in figure 2.13. The

antenna is fed using a microstrip transmission line. The cross slot length and tuning stub length are optimized by [19] for (158 MHz) to be $30mm, 8.5mm$ respectively. This design promise LHCP, and for another desired frequency the cross slot length and tuning stub length have to be optimized again.

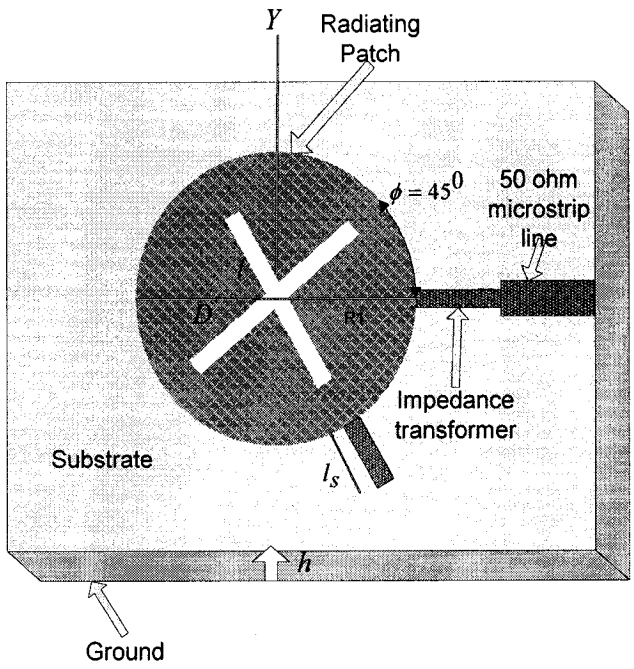

Figure 2.13: Geometry of a circularly polarized circular microstrip antenna with a cross slot and tuning stub [19]

2.5.4.3 Ring Circular Patch Antenna

A ring circular patch antenna generates the CP radiation by adding two inner stubs as shown in figure 2.14. The feed is a microstrip transmission line printed on a different substrate and fed the antenna by a coupling from the open end placed underneath the center of the patch [5]. The inner stubs are optimized for CP radiation and it is given by detail in [5].

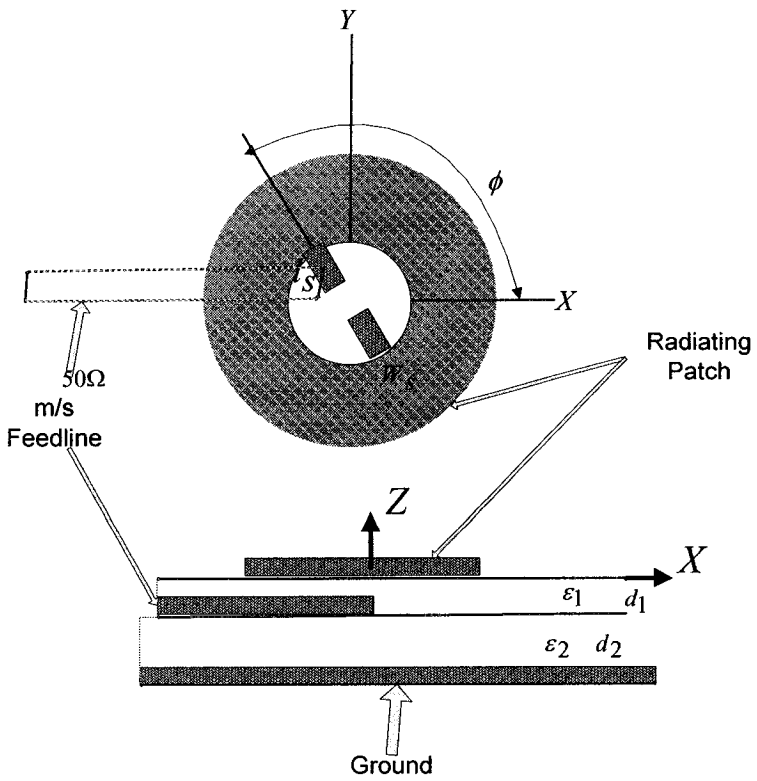

Figure 2.14: Geometry of a circularly polarized ring circular microstrip antenna with tuning stubs

To increase the axial ratio bandwidth of a single element, a sequential rotate array technique is used. The antenna elements are physically rotated relative to each other as shown in figure 2.15. To compensate the rotation, the feed phase is adjusted to each element [5]. Phase shifting between the elements is generated by adding appreciate lengths of a microstrip line.

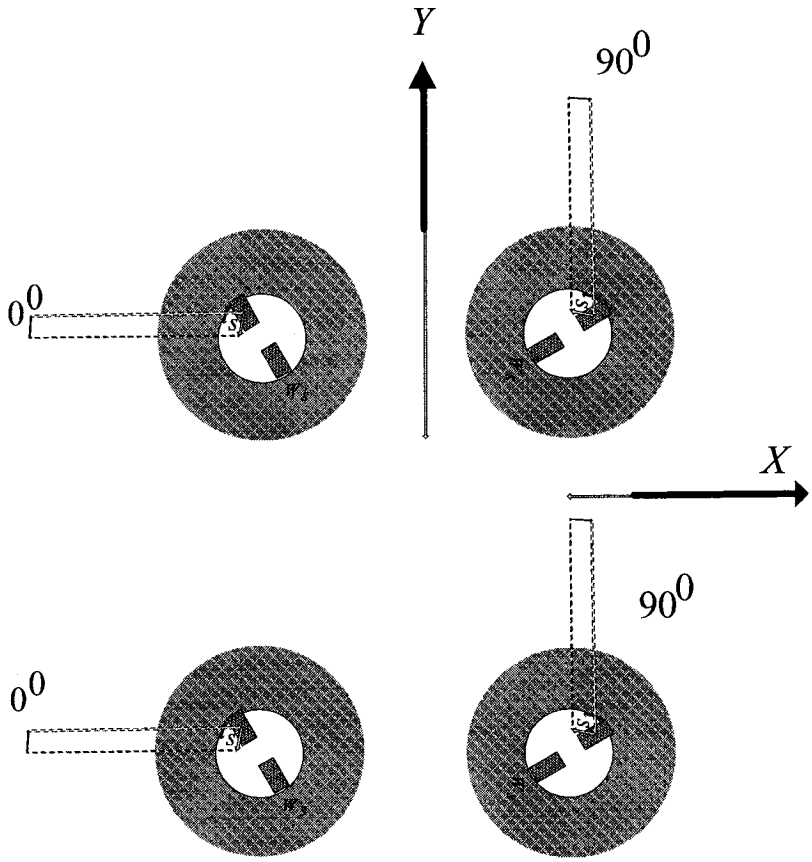

Figure 2.15: Sequential rotated array for a wide band axial ratio

2.5.5 Design with a Bent Tuning Stub

This design is used to generate CP using a circular microstrip patch antenna with symmetric cross slots implanted at the center of the patch. The CP operation is produced using a bent tuning stub aligned along the patch boundary. The length of a tuning stub is optimized in [20] as shown in figure 2.16. The antenna is fed by a coupling slot in the ground plane. Sense of polarization depends on the angle α for the coupling slot. If $\alpha = 45^0$, the antenna is RHCP, and if $\alpha = 178^0$, the antenna generates LHCP radiation.

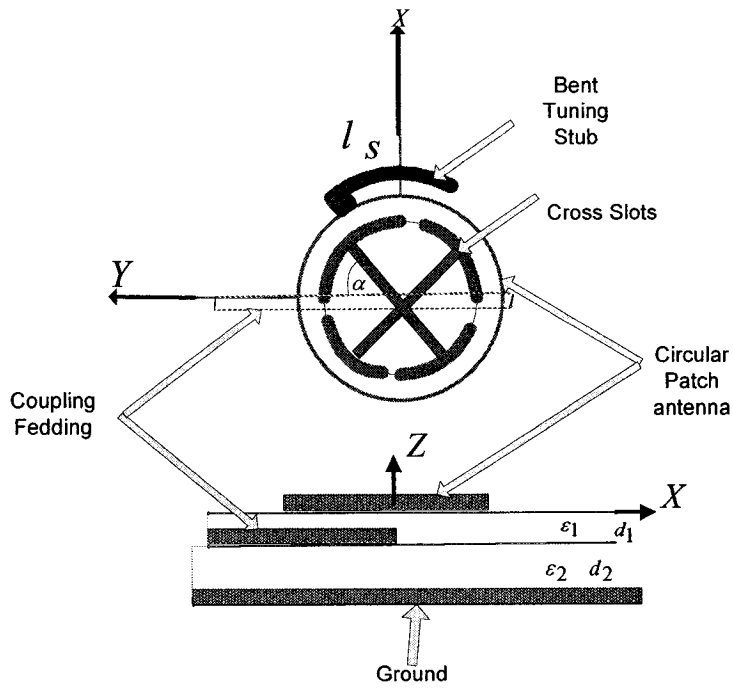

Figure 2.16: Geometry of a circular microstrip patch with a modified cross slot and a bent tuning stub

2.6 Dual band Operation Antennas

Some applications require two far apart operating frequencies that might need two separate antennas. Dual frequency patch antennas are an alternative to separate antennas. Also, dual frequency patch antennas are used instead of large bandwidth antennas. Dual frequency applications can arise in vehicular- satellite communication systems where low cost antennas with an almost isotropic pattern over the upper hemisphere are needed. These demands match the characteristics of patch antennas, especially in synthetic aperture radar (SAR), where the trend of a SAR antenna in the future generation is to cover at least two of three bands with a dual frequency antenna [21].

2.7 Dual band Microstrip Antennas

Dual band microstrip antennas are generally of three types, which are discussed in the following sub-section.

2.7.1 Orthogonal Mode Dual Frequency Patch Antennas

The simplest way to operate the antenna at dual-frequency is to use a rectangular patch to create TM_{10} and TM_{01} modes (using a single or a double feed), and then separate them. This technique is presented with details in [22]. Also, dual-frequency can be produced using slots. Figure 2.17 shows different patch shapes which are used for this technique.

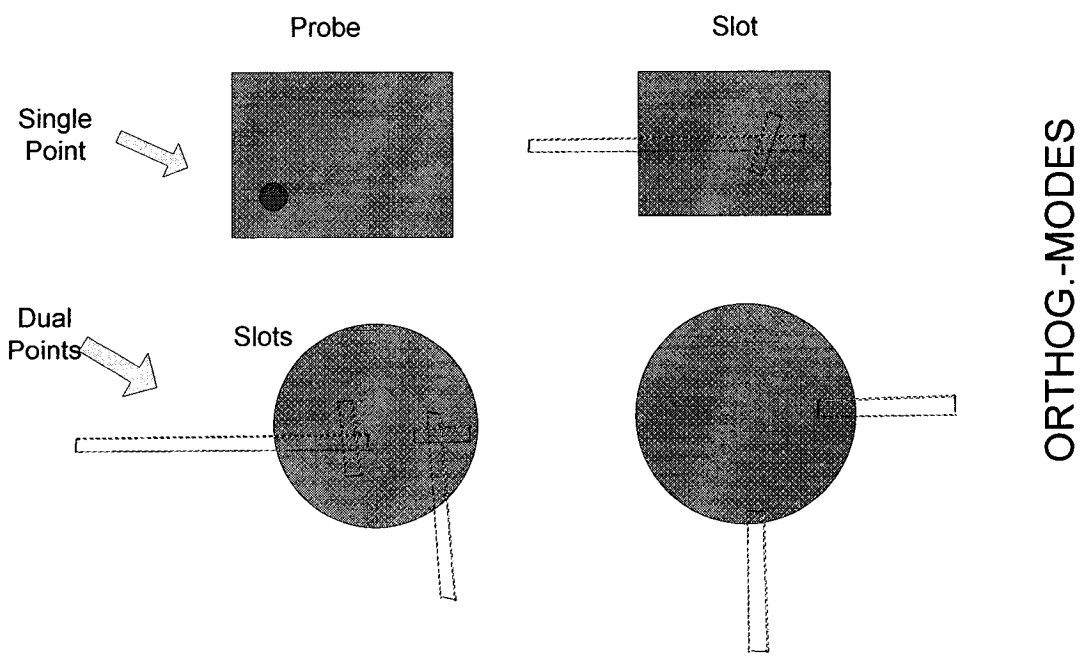

Figure 2.17: Dual frequency patch antennas

2.7.2 Multi Patches Dual Frequency Antennas

Dual-frequency can also be generated using multiple radiating patches, each of them radiated at a different resonance frequency. This type of antennas can be multi layer stacked patches fed by a coaxial cable or a coupling feed. The antenna patches can be circular [23], rectangular [24], or triangular [25] patches. The same concept can also be used to design microstrip antennas with a wide bandwidth in a single band operation.

Multi-frequency antennas can also be obtained by printing more resonators on the same substrate as shown in figure 2.18 and one example of this design with detail is given in [25].

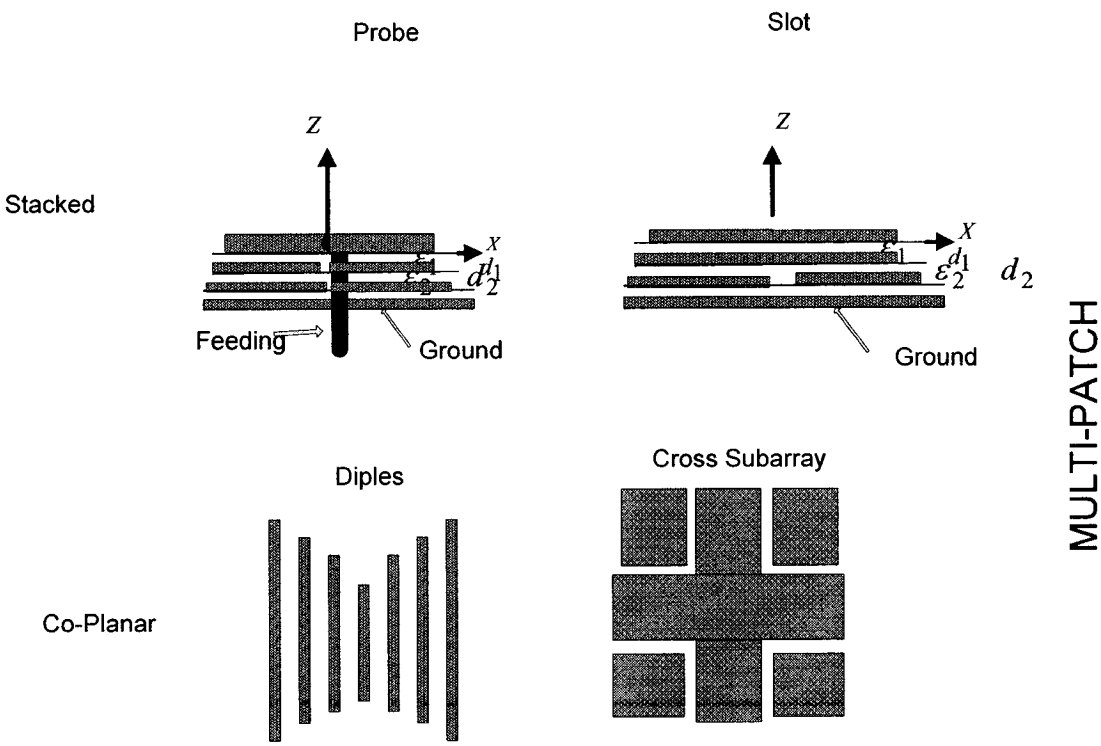

Figure 2.18: Dual frequency patch antennas

2.7.3 Reactively Loaded Patch Antennas

This is a common technique that use for generating dual-frequency operation by introducing a reactive loading to a single patch edge such as a notch, slots, or pins as shown in figure 2.19. This technique can be implemented using rectangular [26], circular [27], or triangular [28] patches.

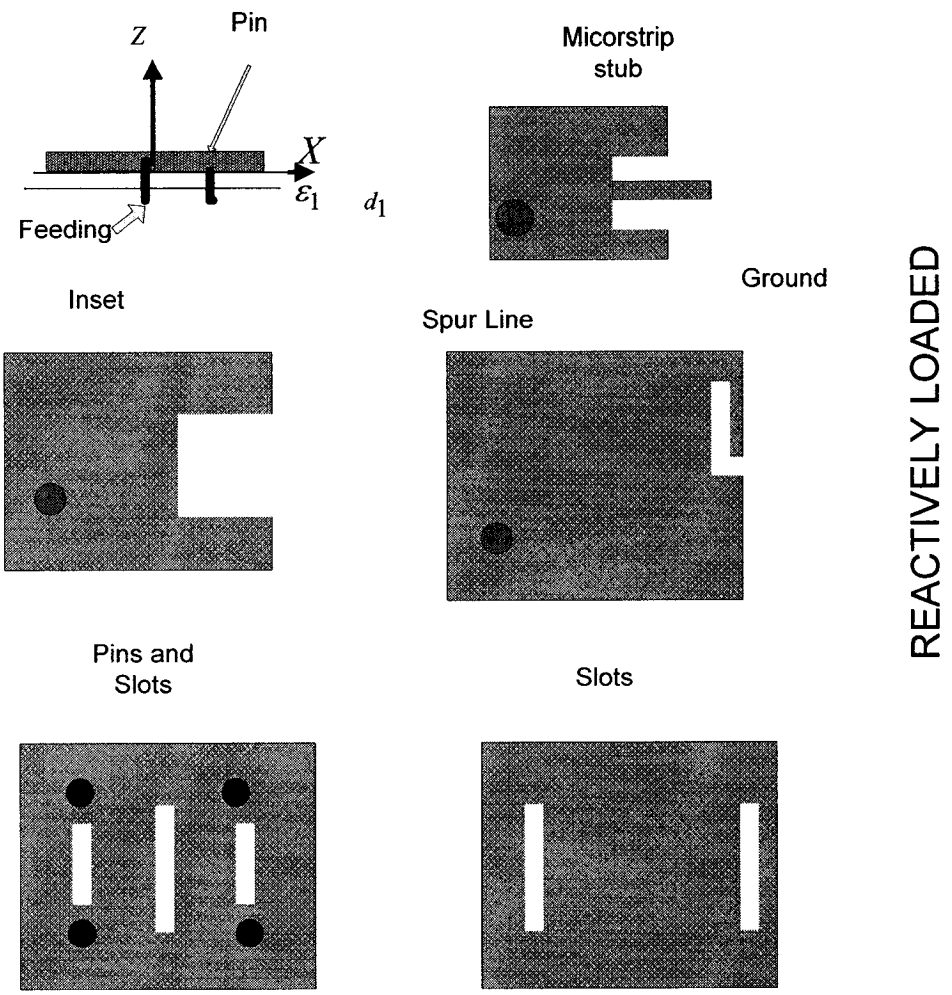

Figure 2.19: Dual frequency patch antennas

2.8 Full Wave Analysis of Microstrip Antennas

For a given source, antenna analysis generally starts with the calculation of electrical and magnetic fields radiated by an antenna. Once fields are calculated, many parameters that characterize the performance of antennas such as radiation pattern, power intensity, directivity, gain, polarization, efficiency, input impedance, and bandwidth can be found.

To minimize the limitation of approximate models that are used to analyze microstrip antennas such as a cavity model, and a transmission line model, the full wave technique has been used to analyze microstrip antennas. The principle of this technique is that: the substrate and a ground plane are infinite, and then applying proper boundary conditions on the patch antenna. The boundary conditions together with specialized Green's function lead to an integral equation that may be solved by numerical techniques such as the method of moment (MOM). Full wave analysis gives a very good solution compared with other techniques that are used to analyze microstrip antennas [29]. Full wave analysis can also be applied to any shape of antenna.

2.9 Numerical Technique for Antenna Analysis

Depending on the electrical size of antennas; there are two categories of electromagnetic wave computational methods; low frequency methods, and high frequency methods. Integral equation (IE) methods and partial differential equation (PDE) methods are developed for antennas with small electrical sizes as shown in figure 2.20. This technique requires a large memory and fast CPU for accurate modeling of large

antennas. When the size of the antenna is large the geometrical theory of diffraction (GTD) and physical theory of diffraction (PTD) are used to analyze these antennas as shown in figure 2.20 [30].

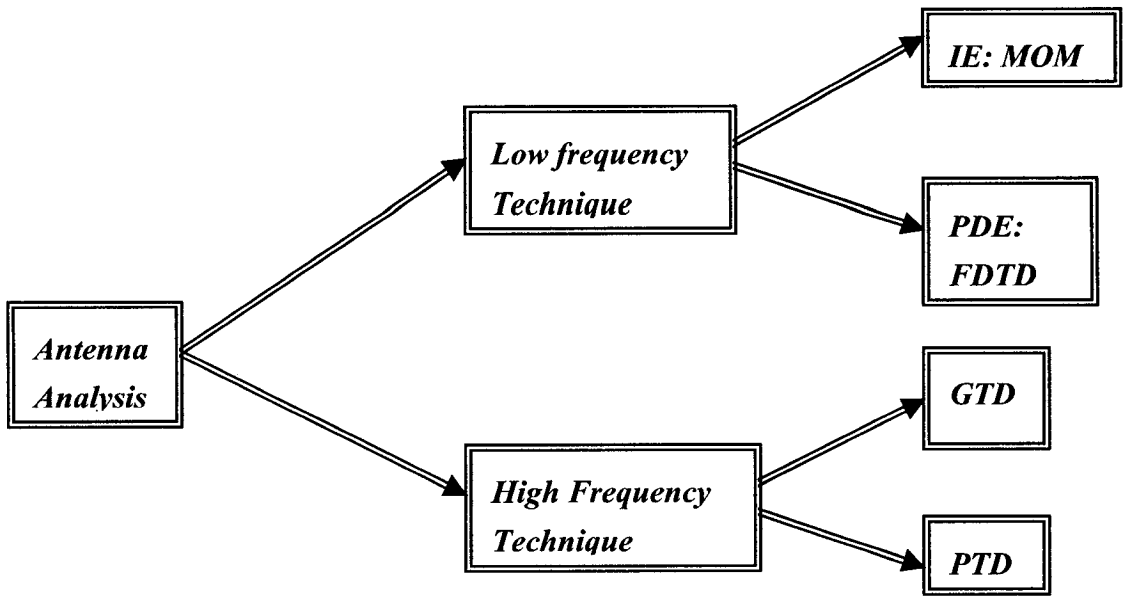

Figure 2.20: Computational methods for antenna analysis

Numerical electromagnetic methods compute fields that:

1- obey Maxwell's equations

2- satisfy proper boundary conditions

3- satisfy all excitation conditions

MOM transforms the continuous integral or differential equations into an approximate discrete formulation that requires either the inversion of a large matrix. Also, there are many ways to discretize an electromagnetic problem. In this thesis the MOM is used.

2.10. Integral Equations and Method of Moment

A popular formulation for the analysis of microstrip antennas is based on the electric field (mixed potential) integral equation:

For a perfect conductor of microstrip antenna as shown in figure 2.21, the total tangential electric field is given by [31]:

$$e_z \times E^{tot}(r) = e_z \times \left\{ \mathrm{E}^{\mathrm{d}}(r) + E^{e}(r) \right\} \tag{2.11}$$

The total electromagnetic field is the sum of the excitation fields E^e and diffracted fields E^d.

$$E_t^e(r) = jw \iint_S \overline{\mathbf{G}}_A\left(r/r'\right).\mathbf{J_S}\left(r'\right)ds' + \nabla t \iint_S \overline{G}_V\left(r/r'\right)\nabla t.\mathbf{J_S}\left(r/r'\right)ds' \tag{2.12}$$

In (2.12), $\mathbf{J_S}$ is the unknown surface current, r is the field point, and r' is the source point.

$\overline{\mathbf{G}}_\mathbf{A}$ and $\overline{\mathrm{G}}_\mathrm{V}$ are the dyadic Green's functions for the vector potential and scalar respectively. Details derivation and expression for $\overline{\mathbf{G}}_\mathbf{A}$ and $\overline{\mathrm{G}}_\mathrm{V}$ are given in [31]-[32]. The integral equation give by (2.12) can be solved using the MOM.

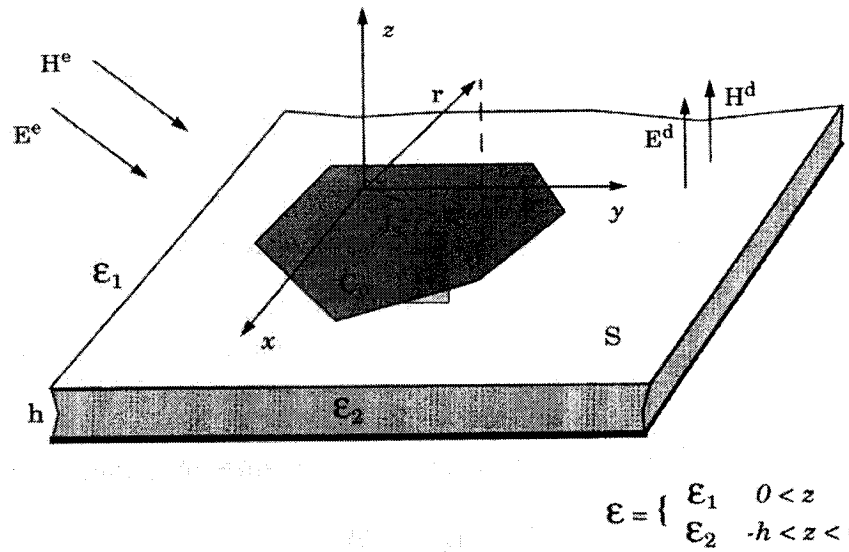

Figure 2.21 Microstrip structure with excitation [32]

MOM is called by different names. It is called the method of projection or the petrov-Galerkin method [29]. The name "method of moments" has its origin in Russian literature. The method owes its name to the process of taking moments by multiplying by appropriate weighting functions and integrating [29].

In the narrow sense, MOM is the method of selection for solving problems stated in the form of an electric field integral equation (EFIE) or a magnetic field integral equation (MFIE).The purpose of MOM is to find approximate solutions to Maxwell's equations that satisfy boundary conditions. In other words, the MOM must solve an integral equation subject to specific conditions. The fundamental idea of MOM is to transfer a functional of equation to a matrix equation and then solve the matrix equation using well known techniques. The MOM has been applied successfully for wide electromagnetic problems such as microstrip patch antennas, scattering problems, wire antennas, and its array, and analysis of microstrip transmission lines feeding [29]-[33]. The outline of generalized MOM is shown in figure 2.22

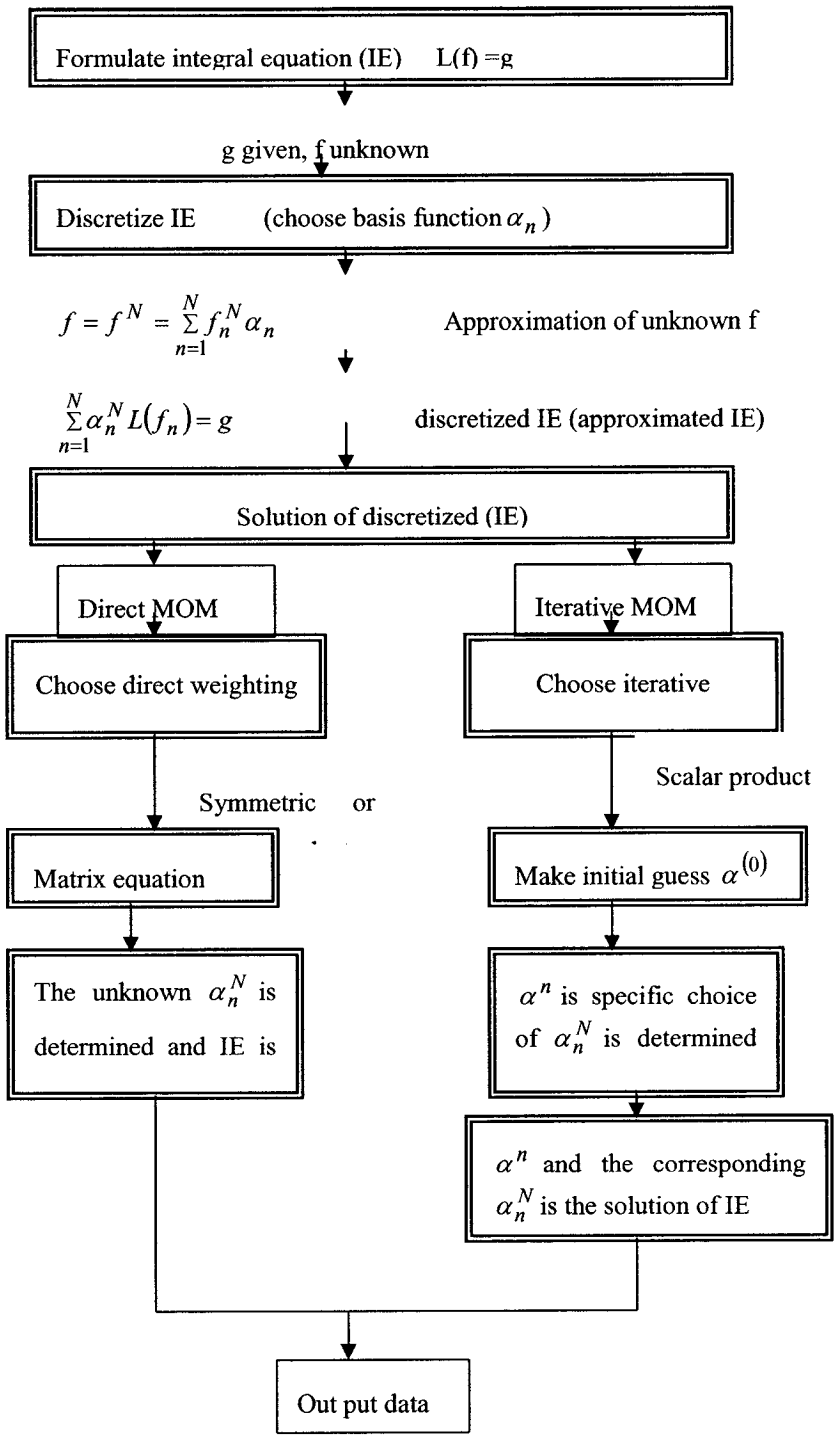

Figure 2.22: Outline of generalized MOM

A continues integral equation such as (2.12) can be written in the form:

$$L(f)=g \tag{2.13}$$

Where L is a known liner operator, g is a known function, and f is the unknown function to be determined. In (2.12), L is the integral operator, f is the unknown surface current, and g is a known source.

The first step in solving a linear operator equation in (2.13) is to project the operator L onto a finite subspace, or equivalently approximating the unknown f in a finite linear space of dimension N as shown in figure 2.23

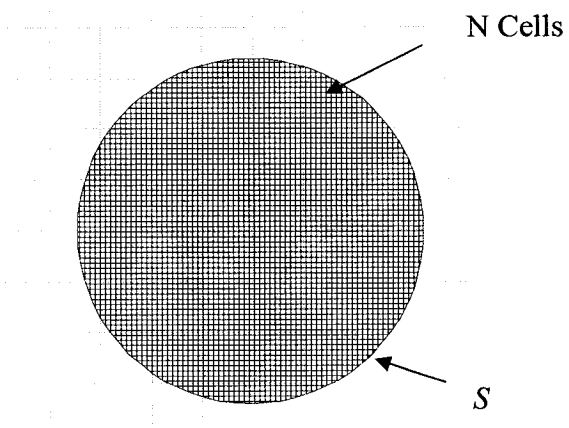

Figure 2.23: 2D finite subspace (circular patch divided into N Cells)

$$f^N = \sum_{n=1}^{N} f_n^N \alpha_n \tag{2.14}$$

Where

f_n, is called expansion function or basis function, and α_n is unknown constant to be determined.

For exact solution, N must be infinite. Therefore, equation (2.14) is an approximation for

the unknown function f.

To approximate the unknown function, numerical methods use different forms of the expansion function. In a practical application the expansion function is reduced with a suitable acceptable approximation error that will include a compromise between an accuracy and computational burden. For an exact representation of a function, a complete set of expansion function (an infinite) should be used. A commonly used choice for f is the pulse function and its integer translation. The width of the pulses is selected according to a desired accuracy value and maximum acceptable number of unknowns [34].

Substituting (2.14) into (2.13) and using the linearity of L (2.13) becomes:

$$\sum_n \alpha_n (f_n) = g_n \tag{2.15}$$

The direct MOM is defined by Harrington [29]. The principle of this method is that choosing N weighing functions, or called testing function, and then taking a symmetric or scalar product on equation of (2.15). As a result, N linear equations are generated which are then numerically solved by matrix method for N unknowns:

$$[\alpha_n] = [l_{mm}^{-1}][g_{mm}] \tag{2.16}$$

α_n values are then substituted into (2.14) to find the current distribution and hence the electric and magnetic fields.

The integral equations solution using MOM has been applied by many researchers to solve various types of microstrip antennas. The analysis is valid for patch resonators, feed networks, and array antennas. This method has been applied for a rectangular patch [35]-[37], for printed wire antennas [38], and for an elliptic patch [39].

2.10.1 Mathematical Model of Excitation of Microstrip Antennas

To analyze microstrip antenna it is necessary to determine the impedance matrix and voltage vector g that represents the antenna excitation. A microstrip patch antenna can be fed by a number of excitation sources such as a probe, microstrip transmission lines, and coupling through a microstrip line underneath the patch [1].

2.10.1 Probe feed

Modeling a coaxial probe feed involves two aspects: a model for the probe current, and another model for the junction effect. A survey of various models for probe-fed patches is given in [40]

2.10.2 Microstrip edge feed

The simplest model neglects the microstrip line in the analysis and uses a vertical filament current at the edge of the patch as shown in figure 2.24a. This model does not include the effect of step-in-impedance discontinuity at the microstrip line junction. Another model that includes a finite section of a microstrip feed line, and introduces a series current generator at the feeding point as shown in figure 2.24b [1].

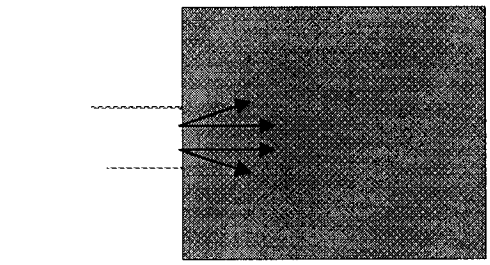

a

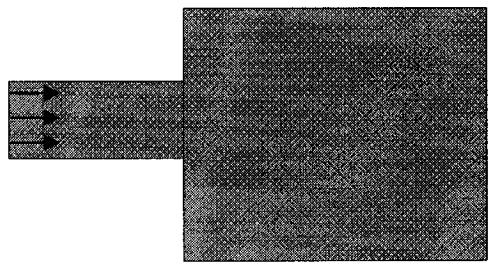

b

Figure 2.24: mathematical model of microstrip excitation
a) Approximate feed model totally neglecting the feed line. b) Approximate feed line partially neglecting the feed line

C h a p t e r T h r e e

Analysis and Design of Single patch Antennas

3.1 Overview

The purpose of this chapter is to introduce a novel design of a circular microstrip antenna with an additional patch excited by a single feed for achieving a dual band operation. Also, introducing a circularly polarized antenna fed by a transmission line microstrip to serve demands of an integrated circuit. A description of the design approaches and geometries of the fabricate antennas are also given.

In the following results, the initial size a circular patch is based on an empirical formula given in Appendix A (A.6). The size is then optimized using full electromagnetic wave simulation tools. For a CP design, an empirical formula based on this work is used.

3.2 Dual Band Microstrip Patch Antenna Design for 2.45 GHz and 5.2 GHz

This design aims to develop a novel design for achieving a dual band operation for ISM band applications. In general, dual band microstrip antennas are of three types: separate microstrip patches (multi patches) coupled to a transmission line, perturbed microstrip resonators where original resonant frequencies are shifted by a geometrical alteration of a basic resonator, or reactively loaded patch antennas.

One of the design steps is to decide an appropriate dielectric substrate of appropriate thickness h and loss tangent. The substrate plays a double role, electrically,

and mechanically. Electrically, it is an integral part of the transmission lines, circuits, and an antenna. Although a thicker substrate is mechanically strong, increases the radiated power, reduces conductor loss, and improves impedance bandwidth, it also increases the weight, dielectric loss, and surface wave loss. A thicker substrate that is grater than 0.11λ does not radiate power due to inductive reactance of the probe feed [1]. The dielectric constant ε_r of the substrate is also an important parameter in the antenna performance. A high dielectric constant ε_r is of great importance. The value of dielectric constant ε_r determines the size. However, low dielectric constant ε_r increases the fringing field, and thus the radiated power. An increase in the substrate thickness has a comparable effect on antenna characteristics as a decrease in the value of ε_r. The desired value of the dielectric constant ε_r for both parameters size of the patch, and radiation patterns is $\varepsilon_r \leq 2.5$. The dielectric losses of the substrate must be a small as possible. A high dielectric loss reduces the antenna efficiency.

In this design a ROGORG RT/5880 Duroid substrate, with thickness 1.575mm and dielectric constantan 2.2 is used. Equation (A.6) is then used to calculate the radius of the patch antenna, shown in figure 3.1, at TM_{11} mode. The additional patch is merged to the main patch and optimized to give good return losses and 3 dB axial ratio for both bands $2.45GHz$ and $5.2GHz$.

3.2.1 Antenna Geometry

The antenna is designed to cover 2.45GHz ISM band applications with RHCP. In addition, a dual band at 5.2 GHZ has been achieved. The antenna compact shape gives it

more advantage in mobile unit applications. As shown in figure 3.1 the designed microstrip antenna patch consists of two circular patches, one is the main patch and the other is the additional smaller patch. The main patch has a radius 23.001 mm. The additional patch is merged with the main circular patch at the coordinate (0.3, 13.2) mm with respect to the main patch's center and its radius is 11.9 mm. The antenna patch is fed by a coaxial cable, and it is located at coordinate (-5, -6.9) mm relative to the main patch's center. The resonance frequency is controlled by changing the radii of both patches, and changing the position of the additional patch as well. The substrate thickness is 1.5757 mm, and the permittivity is 2.2.

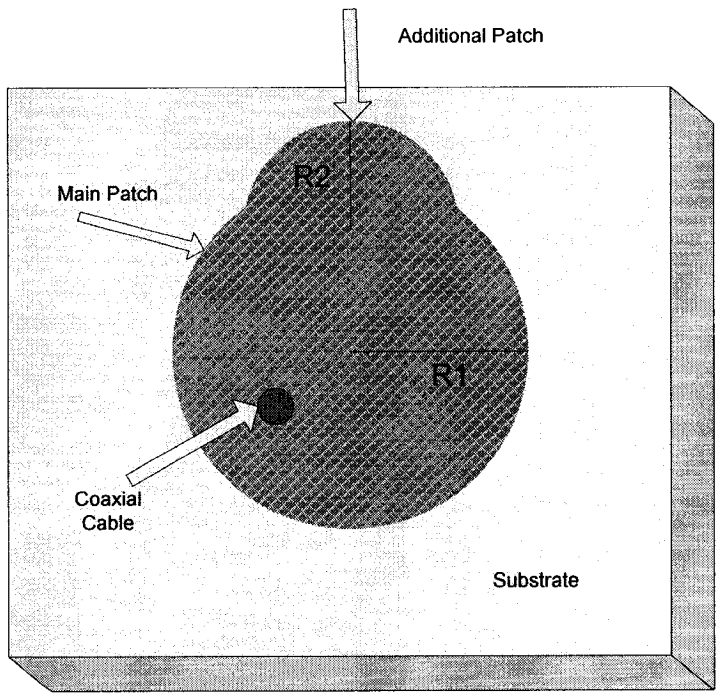

Figure 3.1: Circularly polarized single fed for a dual band microstrip antenna with $\varepsilon_r = 2.2, R_1 = 23.001mm, R_2 = 11.9mm$

3.2.2 Simulated Results

- *Return losses* S_{11}

By selecting the two circular patches in the implemented antenna as shown in figure 3.1 to have slightly different resonant lengths, it is expected that two resonant modes can be excited at frequencies close to each other. Thus an operating bandwidth is greater than that of the design with one circular patch is obtained.

The simulation is carried out using ADS (Advanced Design Systems), and Ansoft HFSS commercial programs. The return losses of the conventional circular microstrip antenna designed at 2.45 GHz is shown in figure 3.2a. Figure 3.2b shows the smith chart for the conventional circular microstrip antenna. Clearly, from figure 3.2b for the conventional circular microstrip antenna, there is no a 'W' shaped link vertex around the center frequency in Smith Chart that means no circular polarization is obtained by a single circular patch antenna. In addition, the bandwidth is around 1.26%.

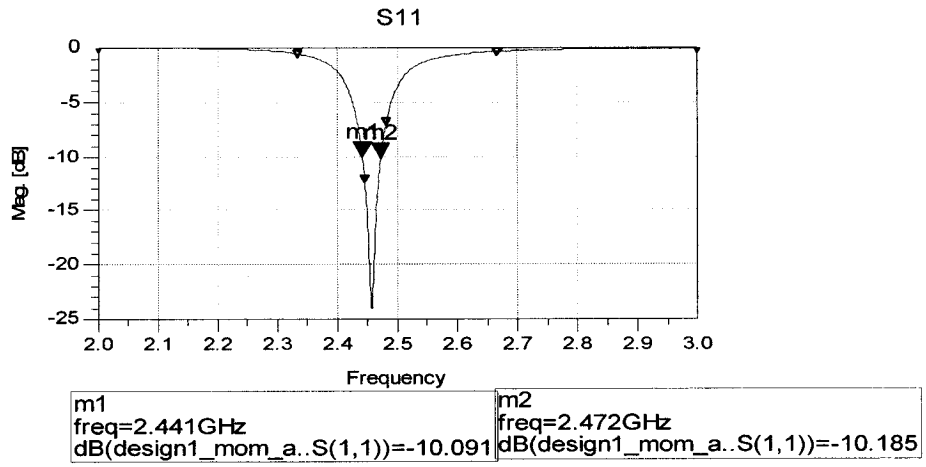

a

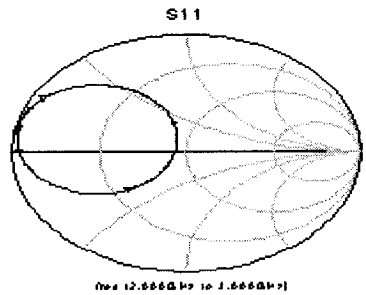

b

Figure 3.2: a) Returns loss of a conventional circular microstrip antenna. b) Smith chart of S_{11}

The return loss of the implemented antenna that is shown in figure 3.1 is given in figure 3.3, a, b. Figure 3.3a shows the calculated and measured return losses (S_{11}). The difference between the simulated and measured results is due to the hand fabrication of the patch which means the size of the patch antenna is not exactly matched between the theory and fabrication. The antenna is resonating at 2.45 GHz, and 5.2 GHZ. At the resonance frequency 2.45 GHZ the return loss is better than -24 dB which is basically a very good value, and the bandwidth of input impedance (BW) is around 4.5% which is 3.75 times the bandwidth for the conventional circular microstrip antenna.

In the other operating band, the antenna is resonating at 5.25 GHz instead of 5.2 GHz, and the return loss at this frequency is around -15 dB which basically is an acceptable value. The input impedance Smith Chart results in figure 4.3b show a 'W' shaped link vertex around the center frequency. This means that the antenna is generating circular polarization.

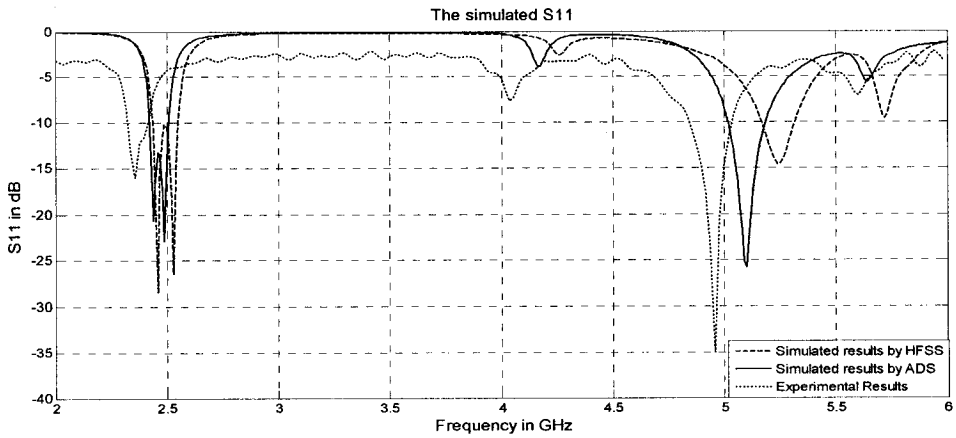

a

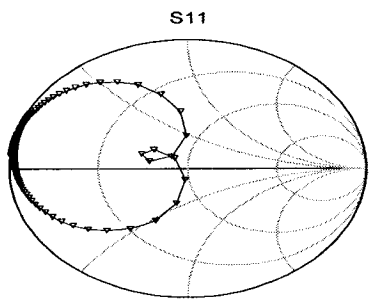

b

Figure 3.3: a) S_{11} results by ADS, HFSS and experiment for the presented antenna.
b) Smith chart of S_{11}

- *Radiation Pattern*

The corresponding far field radiation patterns are simulated and measured. The obtained results are plotted in figure 3.4, and figure 3.5.

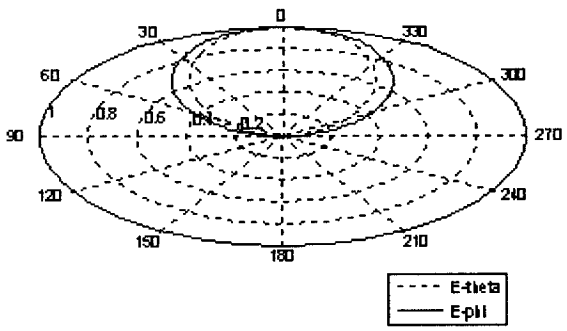

a

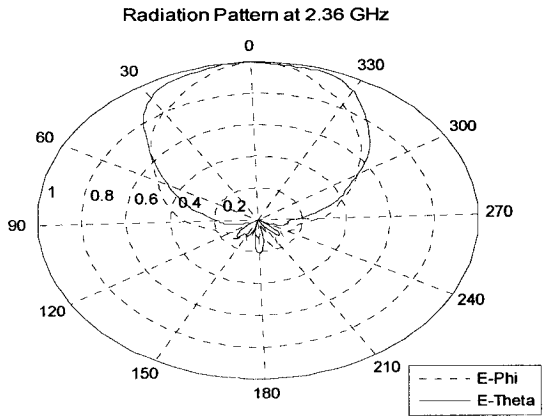

b

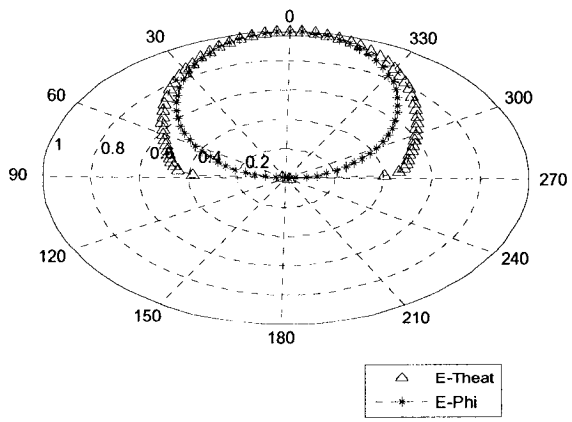

c

Figure 3.4: Radiation patterns of the presented antenna at different frequencies a) 2.43 GHZ, b) 2.36 GHZ, and c) 2.45 GHZ

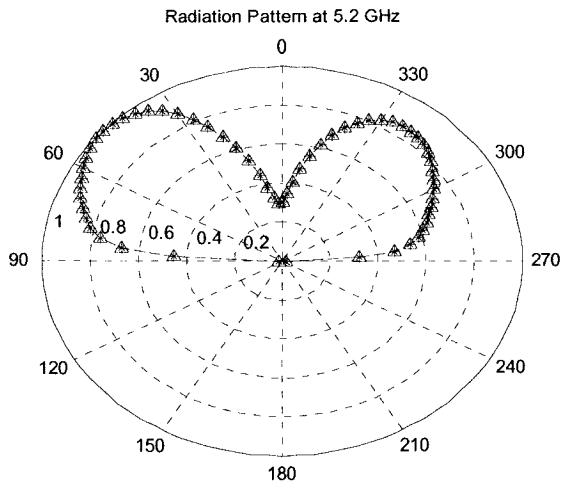

a

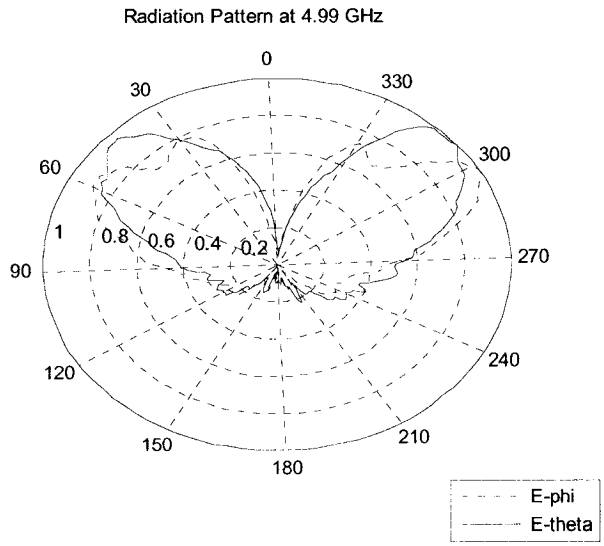

b

Figure 3.5: Radiation patterns of the presented antenna at different frequencies a) 5.2 GHZ, b) 4.99 GHZ

Clearly, the radiation patterns of the antenna are similar to the monopole antenna. This gives the antenna more advantages for a conformal land mobile antenna or as an aircraft antenna for satellite communication applications.

- *Axial Ratio and Directivity*

Figure 3.6 shows the axial ratio as a function of theta(θ). The axial ratio is less than 3 dB over a wide range of theta $\left(-60^0 \; to \; 60^0\right)$ and it various from 0 dB to 2 dB. Figure 3.7 demonstrates the E right and E left (Co-polarization, and cross-polarization). It can be noted that RHCP is the dominant polarization, and LHCP is weaker by about 20 dB. The directivity is computed and is shown in figure 3.8.The directivity is 7.28 dB in the main direction of the beam $\theta = 0$.

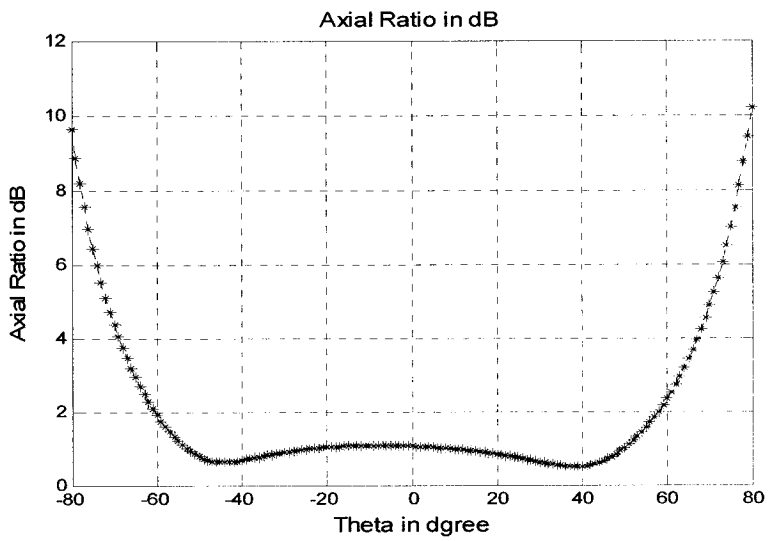

Figure 3.6: Axial ratio of the implemented antenna

with $R_1 = 23.001, R_2 = 11.9mm, and f_r = 2.45GHZ$

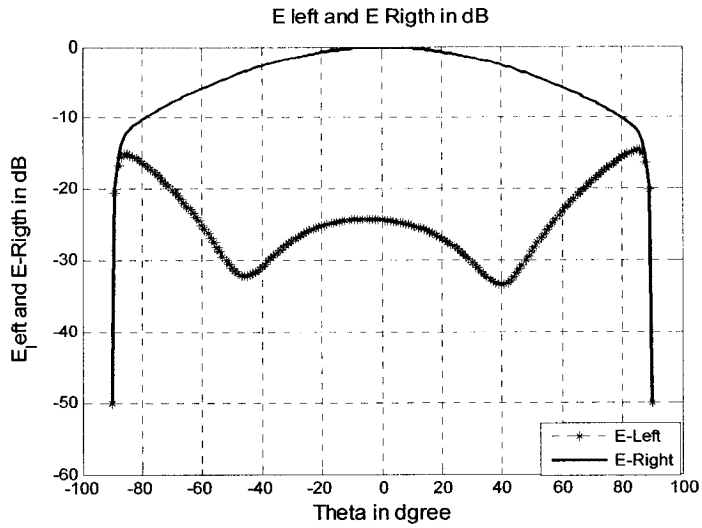

Figure 3.7: E-left and E- right of the antenna at 2.45 GHz

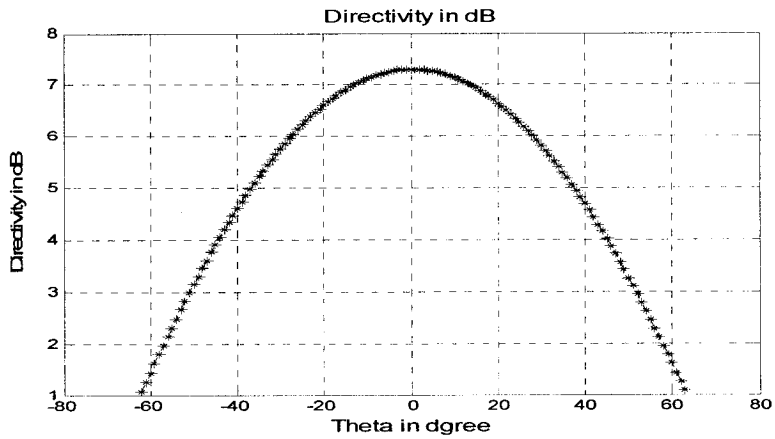

Figure 3.8 Directivity of the implemented antenna with

$R_1 23.001mm, R_2 = 11.9mm$, and $f_r = 2.45GHZ$

3.2.3 Parametric Studies

There are three parameters affecting the performance of the antenna.

1- The radius of the main circular patch.

2- The radius of the additional circular patch.

3- The location of the additional circular patch.

The effects of the parameters on the implemented antenna when the coaxial cable is at (-5, -6.9, 1.575) mm relative to the main patch are shown in figures 3.9 - 3.11. Figure 3.9 demonstrates the effect of the diameter of the main circle. Changing the diameter of the main circle shifts one of the mode frequencies with small effect on the other model. Figure 3.10 demonstrates the effect of the diameter of the additional patch. The simulated results show that changing the diameter of the additional patch shifts one of the mode frequencies; moreover, the other mode is constant. Figure 3.11 shows the effect of the location of the additional patch. The simulated results show that changing the location of the additional patch shifts both resonant frequencies. By changing the diameters of the two patches, the resonant frequencies are shifted to desired frequencies with good 10 dB return-loss impedance bandwidths, and circular polarization at the desired center frequency. After many simulations runs, the following empirical equations are derived. Equations (3.1) and (3.2) give the radii (R1) and (R2) to any desired frequency in the 2-4 GHZ range. And for substrate with thickness $h = 1.575mm$

$$R_1 = \frac{123.975}{\varepsilon_r f_r(GHz)} mm \tag{3.1}$$

$$R_2 = \frac{64.141}{\varepsilon_r f_r(GHz)} mm \tag{3.2}$$

Where, R_1 is the radius of the main circle, R_2 is the radius of the additional patch, f_r the desired resonant frequency in (GHz), and ε_r = dielectric constant of the substrate.

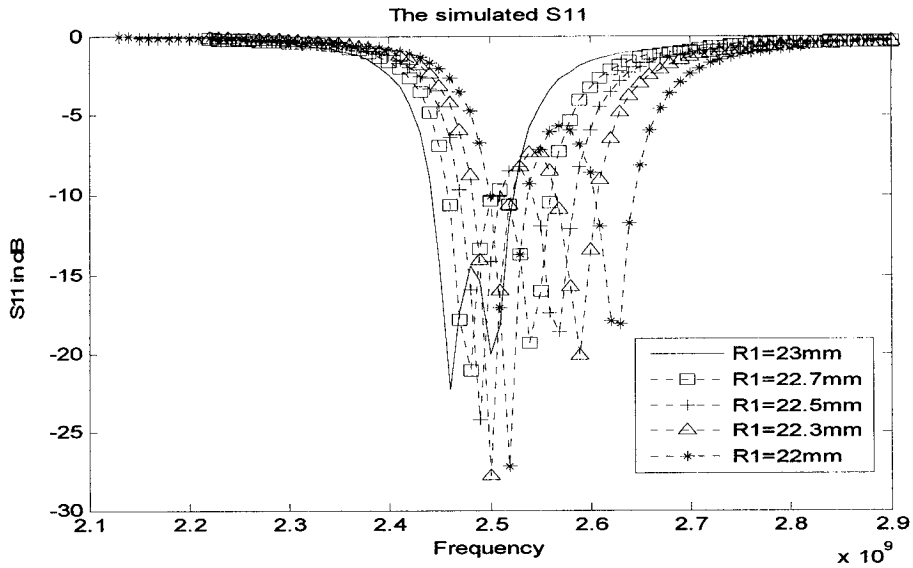

Figure 3.9: Simulated return losses S_{11} of the microstrip antenna as a function of R1, and $R_2 = 11.9$

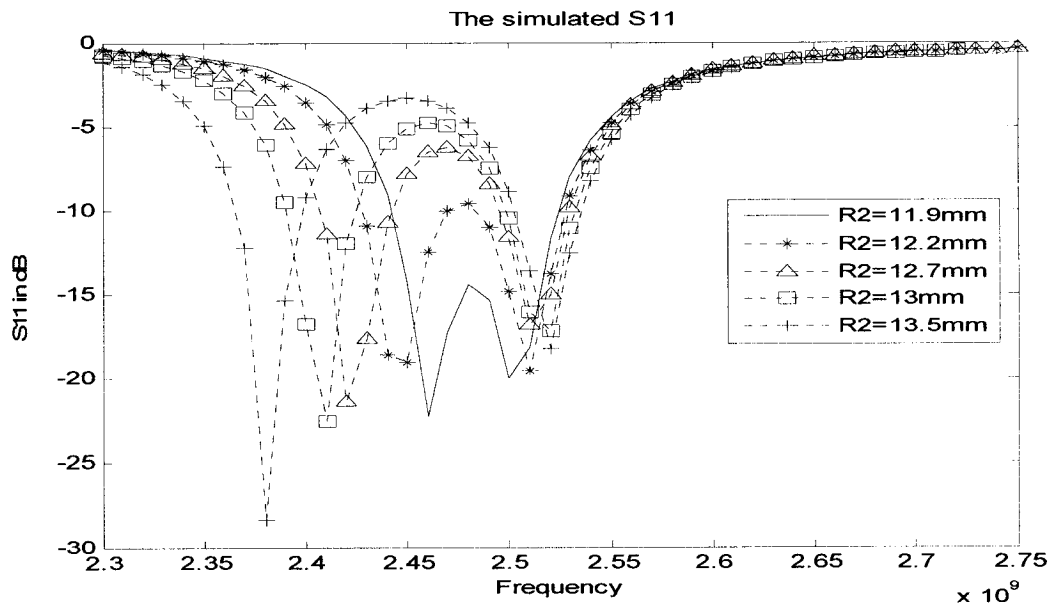

Figure 3.10: Simulated return losses of the microstrip antenna S_{11} as a function of R_2, and $R_1 = 23$mm, f =2.45 GHZ

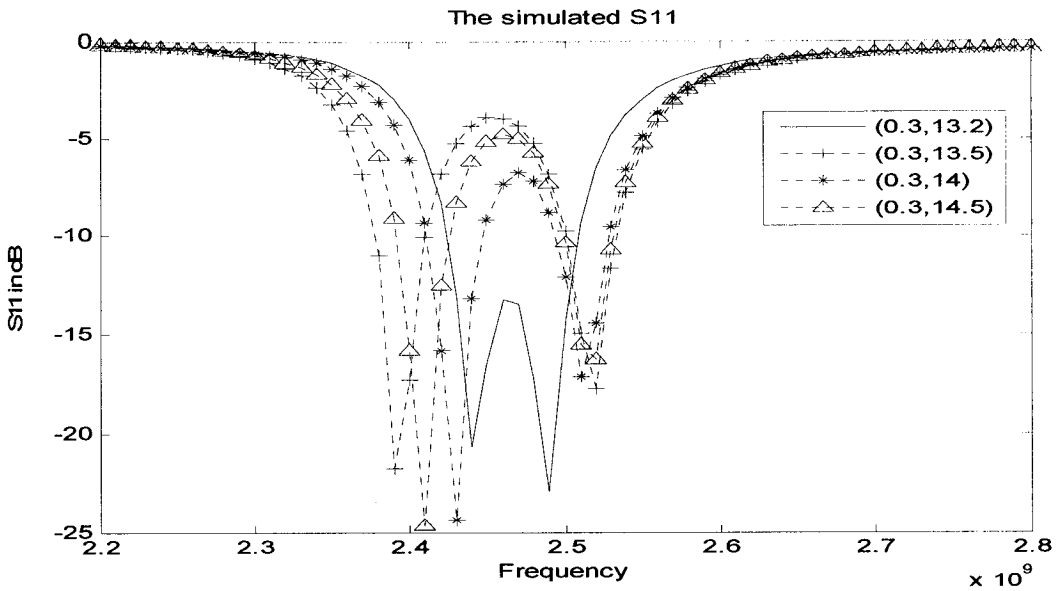

Figure 3.11: Simulated return losses of the microstrip antenna S_{11} as a function of the location of the coupled circle, where R_1=23mm, R_2=11.9mm, f=2.45GHZ

Figure 3.12 shows the simulated result of the return loss(S_{11}) for three types of resonant frequencies (2.2 and 2.4 GHz) achieved by applying equations (3.1, 3. 2).

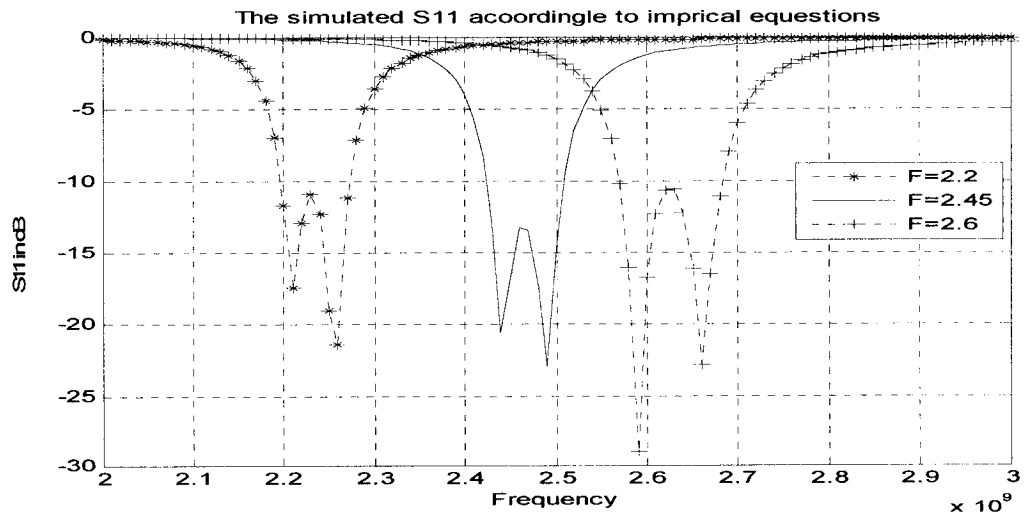

Figure 3.12: Simulated return losses $(S_{11})$of microstrip antennas for three resonance frequencies, f = 2.45, 2.2, 2.6 GHz

3.3 Antenna Design for Left Hand Circular Polarization

To design the antenna with the same characteristics for LHCP the location of a coaxial cable that feeding the antenna is changed to another side. This generates two components with different phase (90^0). The new coordinate of the coaxial cable is (5, 6.9) mm. the antenna is presented in figure 3.13

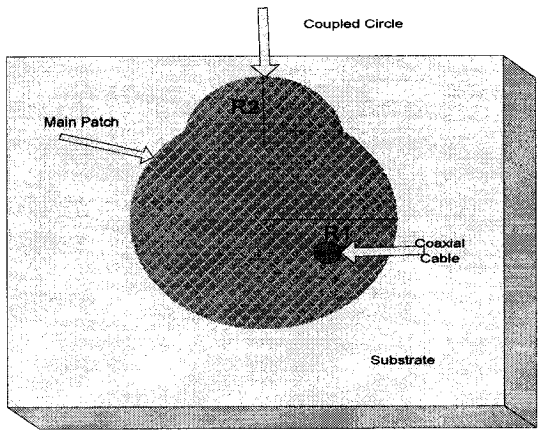

Figure 3.13: Circularly polarized single fed for a dual band microstrip antenna with left hand CP, and $\varepsilon_r = 2.2, R_1 = 23.001mm, R_2 = 11.9mm$

The co-polarization and corss-polarization of the left hand circularly polarized antenna are shown in figure 3.14. The dominant polarization is LHCP.

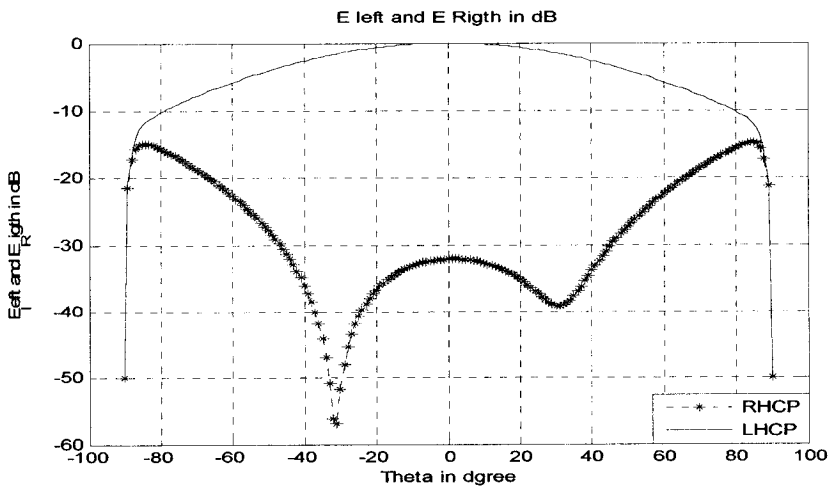

Figure 3.14: E-left and E- right of the antenna

3.4 Single Element Microstrip Patch Antenna Fed by a Microstrip Transmission Line to Cover 2.45 GHz

The single feed circular patch antenna is designed using a RT/5880 Duroid with $\varepsilon_r = 2.2$ and a dielectric thickness of $h = 1.575mm$. First step is to determine the radii of the main patch, and the additional patch antenna. The size of main patch antenna is calculated by equation (A.6). The additional patch was optimized for good 10 dB return losses bandwidth, and good axial ratio of circular polarization at the center frequency.

3.4.1 Antenna Geometry

The antenna is designed to cover 2.45GHz (for TM_{11} mode) ISM band applications with LHCP. The antenna is compact shape, and it is fed by a microstrip transmission line that gives it more advantage for integration with RF circuits. As shown in figure 3.15 [41], the designed microstrip antenna patch consists of two circular patches, one is the main patch and the other is the additional smaller patch. The main patch has a radius 24.25 mm. The additional patch is directly merged with the main circular patch at the coordinate (10.25, 12.07) mm with respect to the main patch's center and its radius is 10.125 mm. The antenna is fed by a 50 ohm microstrip transmission line and it is connected to the center of the antenna. The input impedance of the antenna is 200 ohm. The quarter wave transform is used to convert 200 ohm to 50 ohm. The quarter wave transform is designed at the center frequency of 2.45 GHz. The width of the quarter wave transform is 1.2mm and the length is 26.2mm. The width of the 50 transmission line is 4.2mm. The resonance frequency is controlled by changing the radius of both, the main and the additional patches, and changing the position of the additional patch as well.

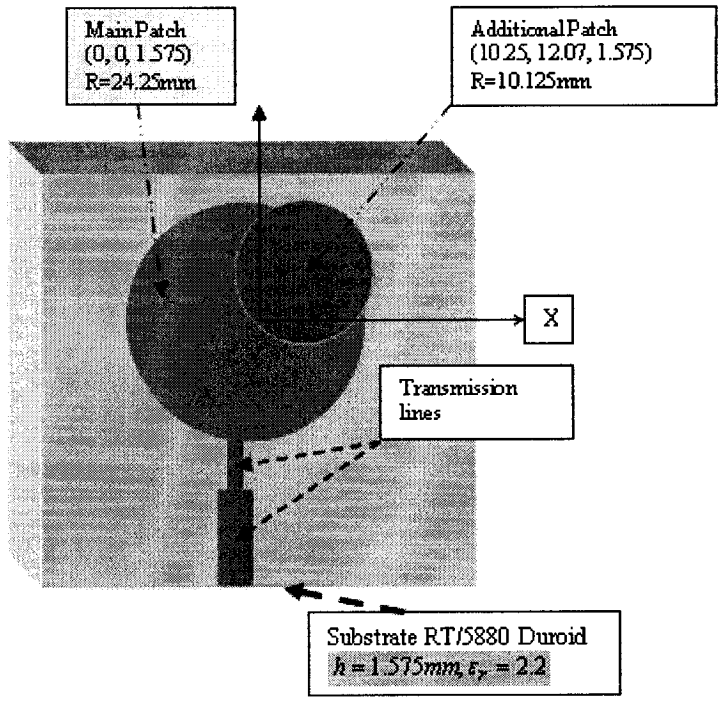

Figure 3.15: Geometry of the designed antenna feeding by a transmission line

3.4.2 Antenna Performance

- *Return Losses*

The return loss of the presented antenna is shown in figure 3.16. Figure 3.16 presents the simulated and measured results of the return losses. The simulated and experimental results are in good agreement. The bandwidth of proposed antenna is about 3.75 times that of a single patch microstrip antenna. The smith chart of the measured impedance is presented in figure 3.17 and it shows "W" shaped link vector around the center frequency.

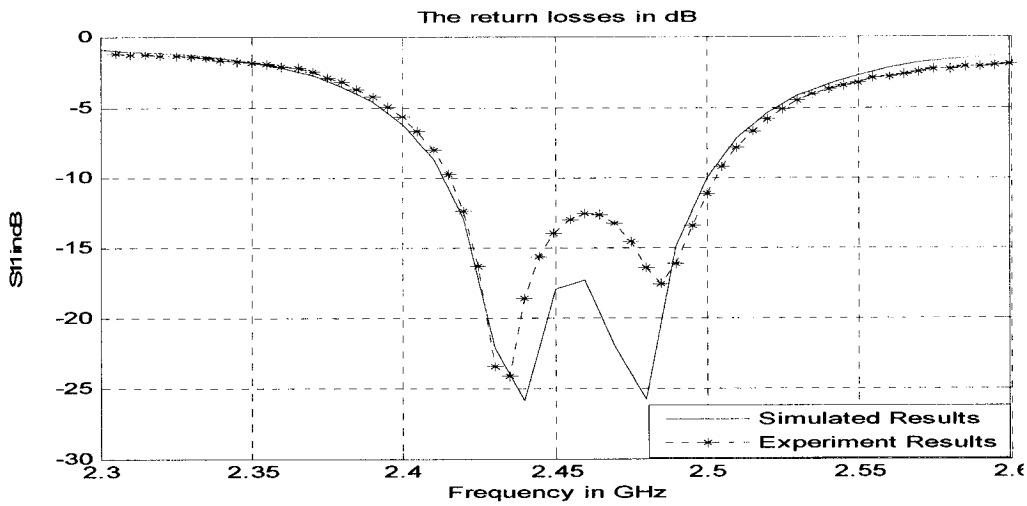

Figure 3.16: Simulated and experimental results S_{11}, for the presented antenna

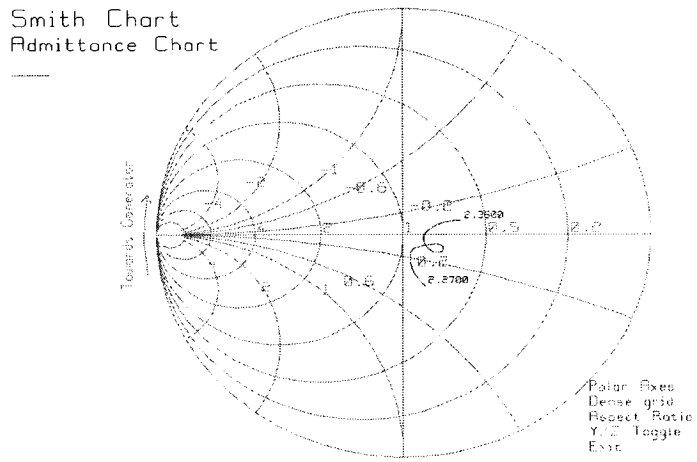

Figure 3.17 Smith chart measured results

- *Radiation Pattern*

For the designed antenna shown in figure 3.15 the corresponding far fields radiation patterns are simulated, and measured. The obtained results are plotted in figure 3.18. Figure 3.18a shows the simulated results of E_θ, and E_ϕ. Figure 3.18b shows the measured and simulated results of radiation pattern E_θ. Figure 3.18c shows simulated results of E_θ, E_ϕ with 45^0 half power beam width of the implemented antenna.

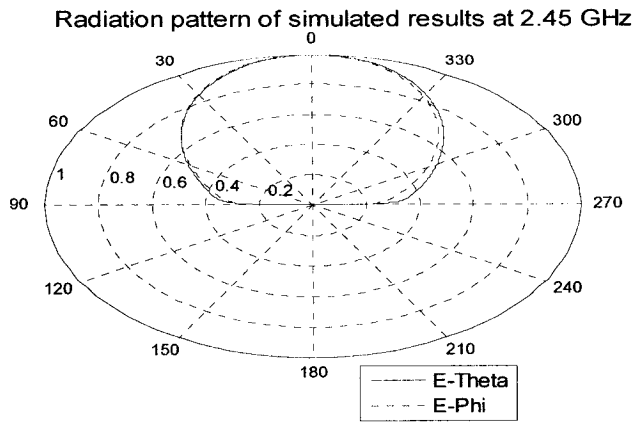

a

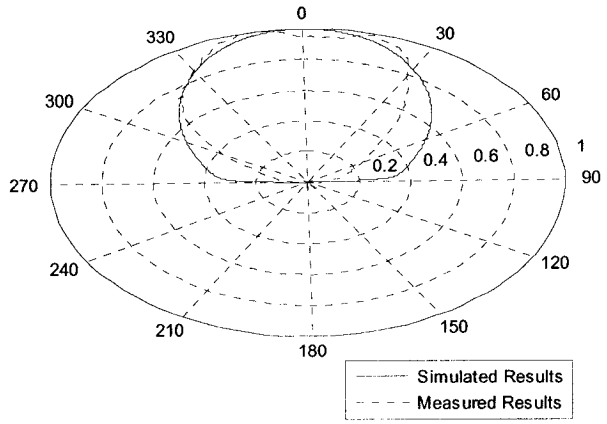

b

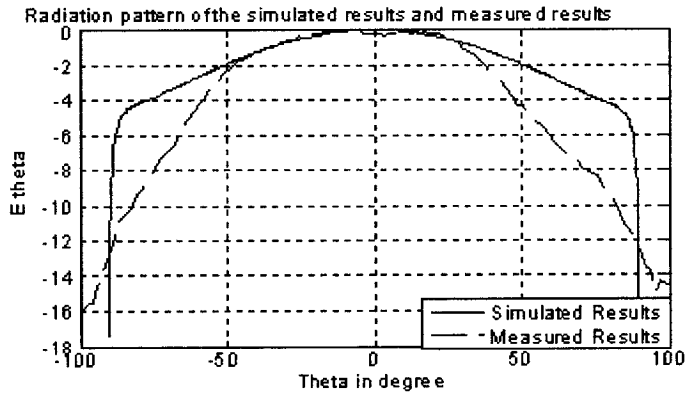

c

Figure 3.18: Radiation patterns of the presented antenna at different frequencies a) 2.45GHz, b) 2.45GHz, & c) 2.47 GHz

- *Axial Ratio*

Figure 3.19 demonstrates the axial ratio as a function of θ when ϕ =0 for different frequencies. The axial ratio is less than 3 dB along a wide range of θ, and it various from 0.9 dB to3 dB. From the graph the axial ratio is less than 3dB over the entire range ($-60^0 to +60^0$).

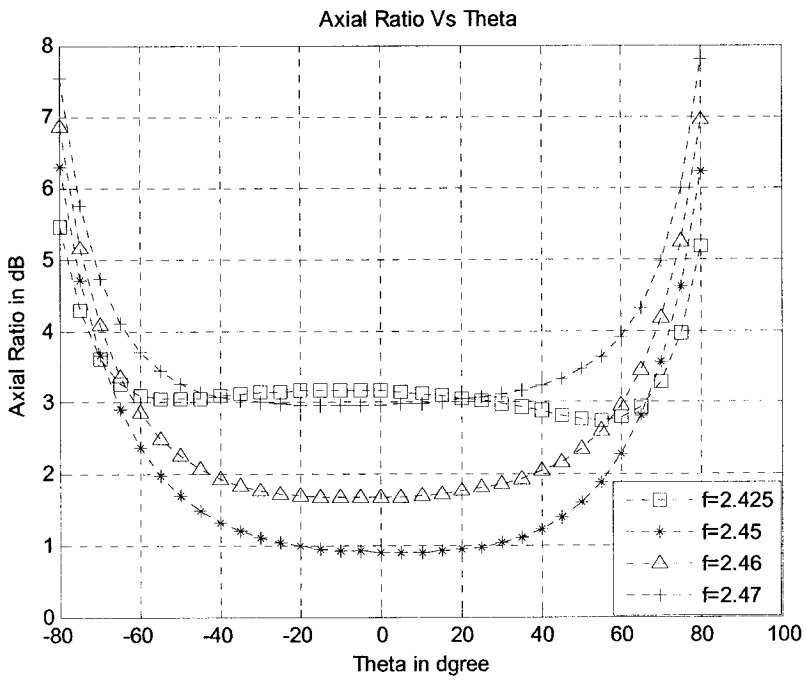

Figure 3.19: Simulated results of the axial ratio as a function of θ

Figure 3.20 shows the axial ratio as a function of the frequency, when θ is 0. The 3*dB* axial ratio bandwidth is about 1.64%.

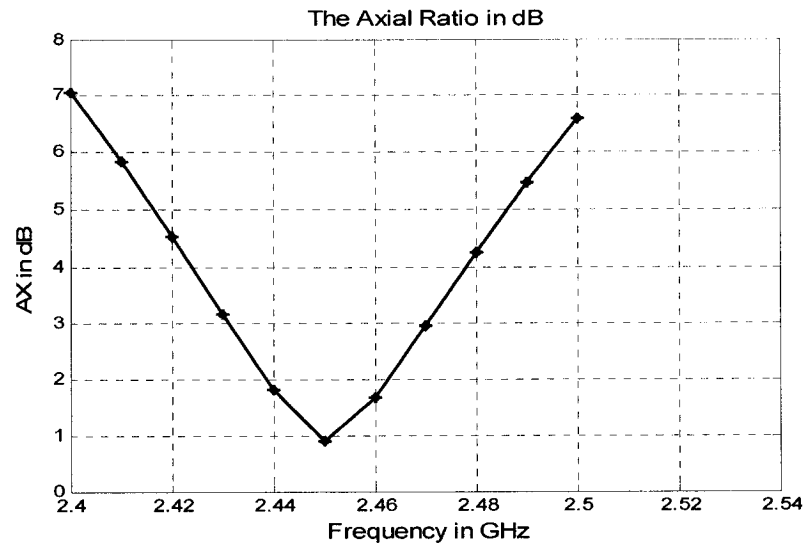

Figure 3.20: Simulated results of the axial ratio as a function of the frequency

- *Directivity*

The directivity is computed and it is shown in figure 3.21. The directivity is 6.93 dB at $\theta = 0, \phi = 0$

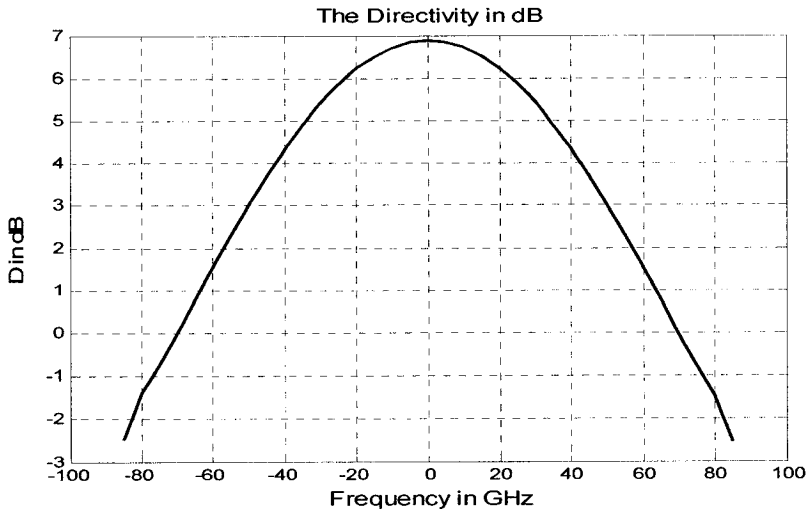

Figure 3.21: Directivity at the center frequency (2.45 GHz)

Figure 3.22 shows the directivity of the antenna as a function of the frequency. From figure 3.22 the directivity is more than 6 dB over the entire bandwidth 2.4 – 2.5 GHz.

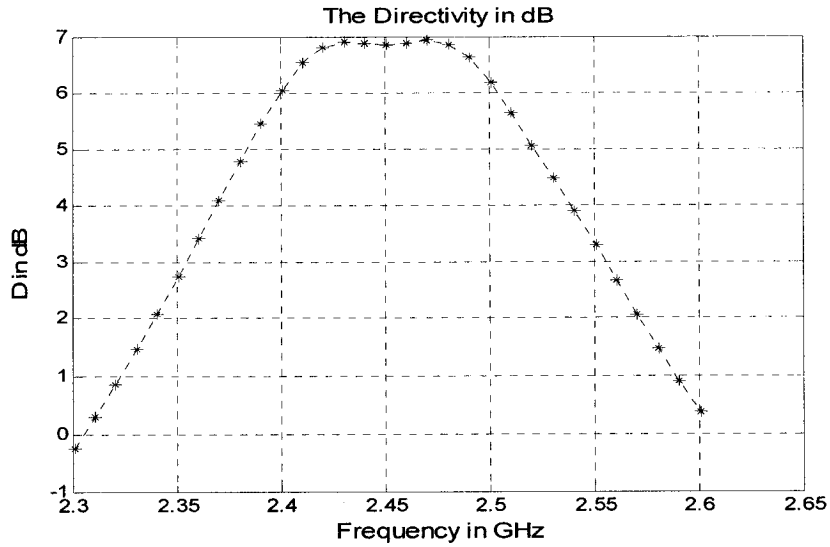

Figure 3.22: Directivity as a function of the frequency

- *Effects of Radii of Main and Additional Patches*

There are three design parameters for the antenna such as radius of the main and additional patch, and location of the additional patch. These parameters affect the impedance bandwidth, and the axial ratio of the antenna. The antenna could be designed at any desired frequency with similar characteristics by selecting appropriate values of radii of main and additional patches. After many simulations runs, the following empirical equations are derived. Equations (3.3) and (3.4) give the radii (R1) and (R2) to any desired frequency in the 2-4 GHZ range for a substrate with thickness $h = 1.575mm$.

$$R_1 = \frac{130.708}{\varepsilon_r f_r(GHz)} mm \tag{3.3}$$

$$R_2 = \frac{54.71}{\varepsilon_r f_r(GHz)} mm \tag{3.4}$$

R_1 is the radius of the main circle, R_2 is the radius of the additional circle, f_r is the desired resonant frequency in (GHz), and ε_r = dielectric constant of the substrate.

3.5 Single Element Microstrip Patch Antenna Design for 5.2 GHz Band

The geometry of the antenna is shown in figure 3.23, a, b. The radius of the main circle is $R_{Main\,Circle} = 10.7mm$, and its orientation with respect to xy coordinate is $(0,0)$. The radius of the small additional circle, which has been merged to the main circle, is $R_{Additional\,Circle} = 6.5mm$, and its orientation relative to the main circle is $(4,4.2)mm$ for LHCP, and $(-4,4.2)mm$ for RHCP.

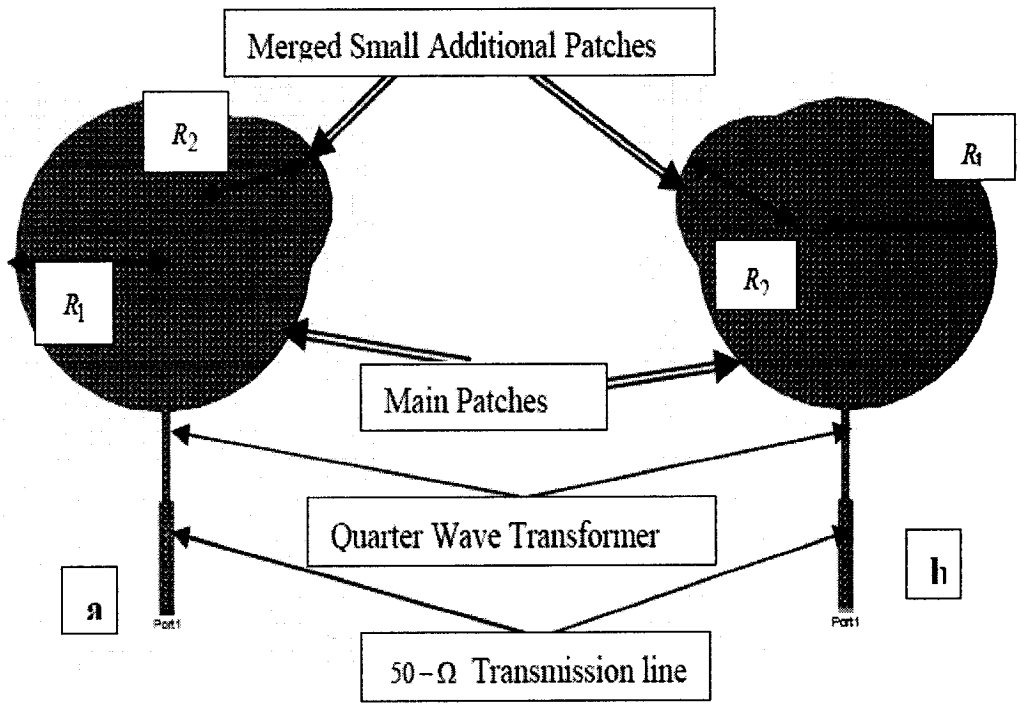

Figure 3.23: Geometry of the proposed antenna. a) LFHCP, b) RHCP

3.5.1 Return Losses and Axial Ratio Bandwidths

Figure 3.24a shows that the input impedance bandwidth is 9.3% for both RHCP and LFHCP. Figure 3.24b shows that the axial ratio bandwidth is 3.5% at $\phi = 0^0, 90^0$. Figure 3.25a, 3.25b show S_{11} and AX versus the radius of the main patch. Changing the radius of the main patch affects the bandwidth quality of the axial ratio, the input impedance bandwidth, and the resonance frequency. Figures 3.26a and 3.26b shows the results of S_{11}, and the axial ratio (AX) as functions of the radius of the additional circular patch. Changing the radius of the additional patch affects the quality of the axial ratio, and causes small effect on the input impedance bandwidth.

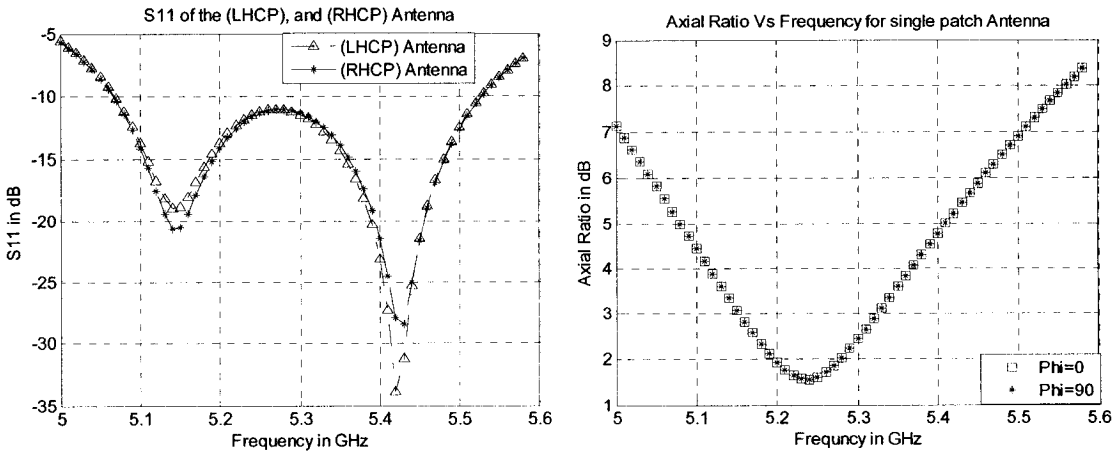

a b

Figure 3.24: a) Return losses. b) Axial ratio of the single patch antenna

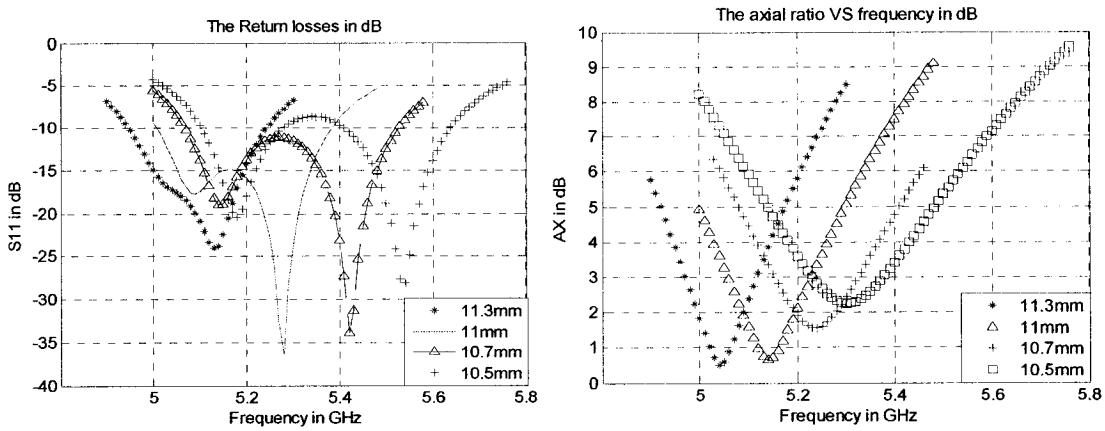

a b

Figure 3.25: a) Return losses. b) Axial ratio as function of the radius of the main circular patch

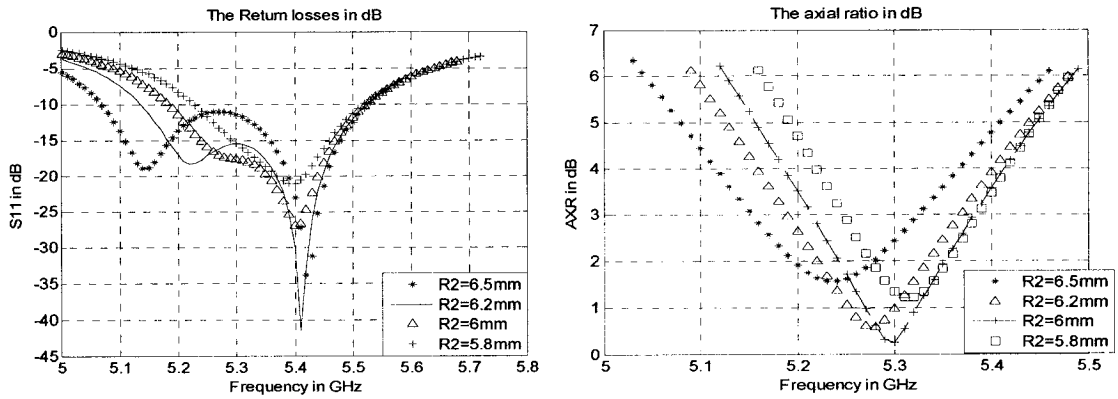

a b

Figure 3.26: a) Return losses. b) Axial ratio as function of the radius of the additional circular patch

C h a p t e r F o u r

Analysis and Design of an Antenna Arrays: Numerical Results

4.1 Overview

This chapter introduces a high gain circularly polarized microstrip antenna array which is designed to serve demands of an industrial and scientific medical (ISM) wireless communication. Also, a sequential rotated array is introduced for a wideband axial ratio. A comparison between a single patch of the designed antenna with a four patches sequential rotated array with orientation of 0^0,90^0,0^0,90^0 is presented.

4.2 Microstrip Patch Antenna Arrays

In some particular applications, such as indoor communications, require wide beams that single patch antennas provide. However, characteristics such as high gain, beam scanning, or steering capability are possible only when patch antennas are combined to form an array. The elements of an array may be spatially distributed to form a linear, planar, or volume array.

In order to be able to design a circularly polarized microstrip patch antenna array the following steps should be made:

1. Design a single patch circularly polarized patch antenna.
2. Design the feed network at the same resonant frequency of the single patch.
3. Form a microstrip patch antenna array with a specific number of elements.

4.3 Design of a Circularly Polarized Uniform Linear Array of Microstrip Patch Antennas at 2.45 GHz

A sixty four elements circular polarized antenna array is designed to achieve more than 20 dB directivity with good axial ratio. A large antenna array can be designed by first investigating the single element to determine an optimal antenna geometry, then by forming a small array that can be integrated into a large array. In this design the, the single antenna is presented in section 3.4.

Arrays can be fed in several different manners such as series feed; a single transmission line is directly coupled to the radiated elements. In this design parallel feeds, generally called corporate feeds, have been used. The feed network divided the input signal into several channels, which individually feeds each of the radiating elements as shown in figure 4.1.

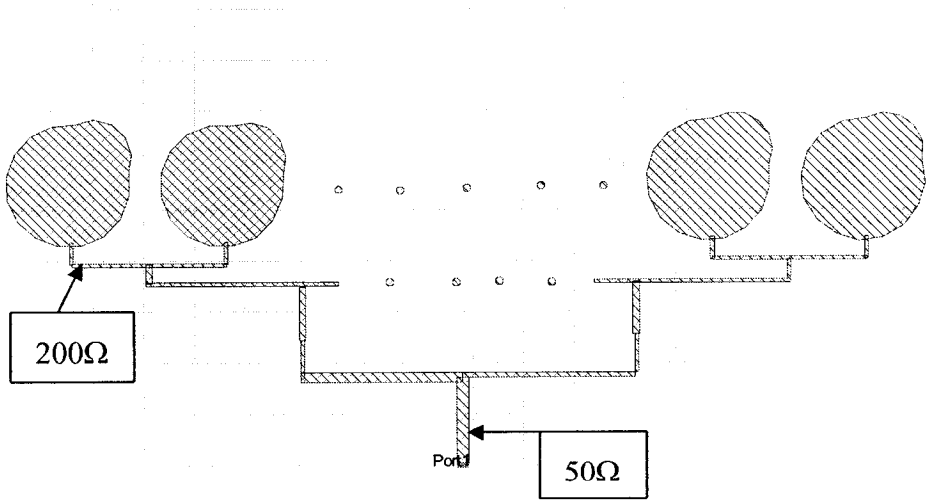

Figure 4.1: Shape of the sixty four elements patch antenna array

4.3.1 Simulated Results of the Sixty Four Elements Patch Antenna Array

Figure 4.2a demonstrates the radiation pattern of the antenna array (E_θ) . The half power beam width $(HPBW)$ is 0.75 degree and the side lop level is -14.9 dB. Figure 4.2b shows the computed directivity of the antenna array, and it is 22 dB. Figure 4.3.a presents the simulated results of return losses, and figure 4.3b shows the axial ratio as a function of the frequency at $(\theta = 0, \phi = 0)$.

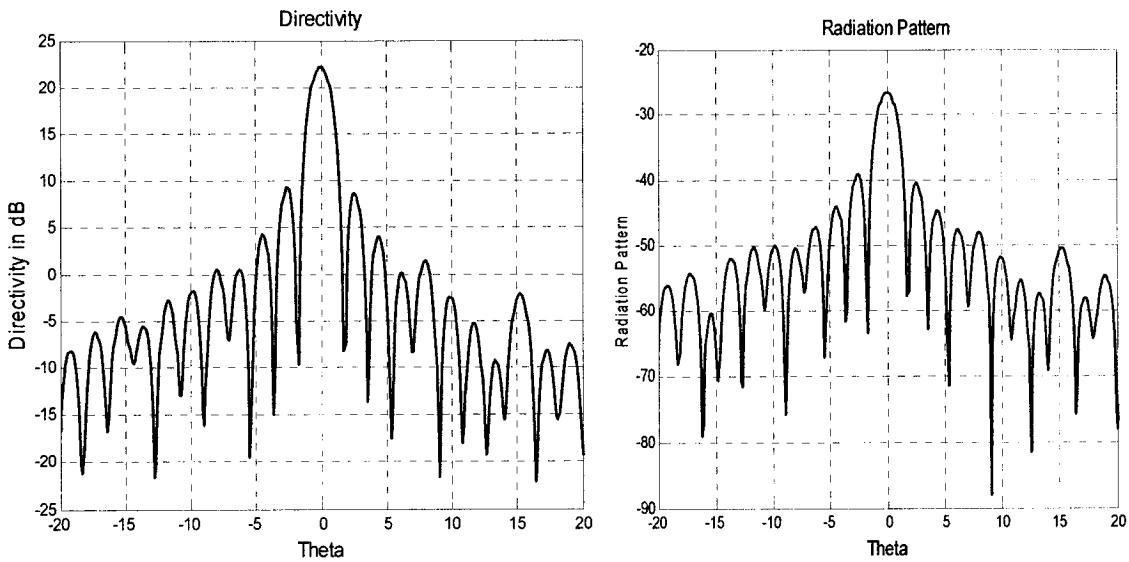

a b

Figure 4.2: a) Directivity of the implemented antenna with $R_1 = 24.25mm, R_2 = 10.15mm$, and $f_r = 2.45GHz$. b) Radiation pattern (E_θ) of the antenna array with $R_1 = 24.25mm, R_2 = 10.15mm$, and $f_r = 2.45GHz$

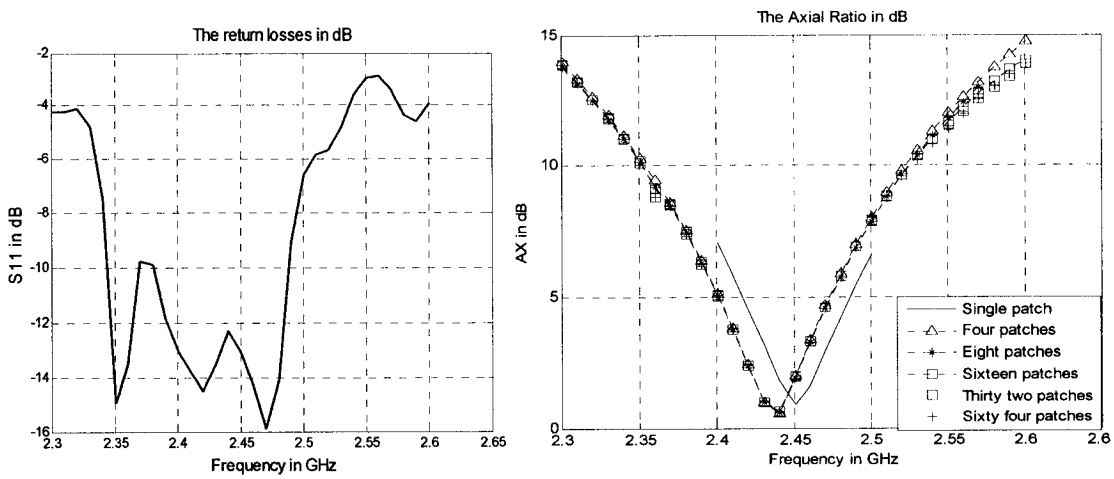

a b

Figure 4.3: a) Return losses of the antenna array with $R_1 = 24.25mm$, $R_2 = 10.15mm$, and $f_r = 2.45GHz$. b) Axial ratio of the single and array antenna with $R_1 = 24.25mm$, $R_2 = 10.15mm$, and $f_r = 2.45GHz$

4.3.2 Effect of the Mutual Coupling on the Axial Ratio of the Patch Antenna Array

Changing the distance between the elements of the antenna array will change the axial ratio of the antenna because the effects of the mutual coupling. Figure 4.4 shows the difference of the axial ratio when the distance between the elements is 0.5λ, 0.7λ, and $0.9\ \lambda$. The axial ratio is less than 1 dB when the distance between the elements is $0.5\lambda < d > 0.7\lambda$ as shown in figure 4.4

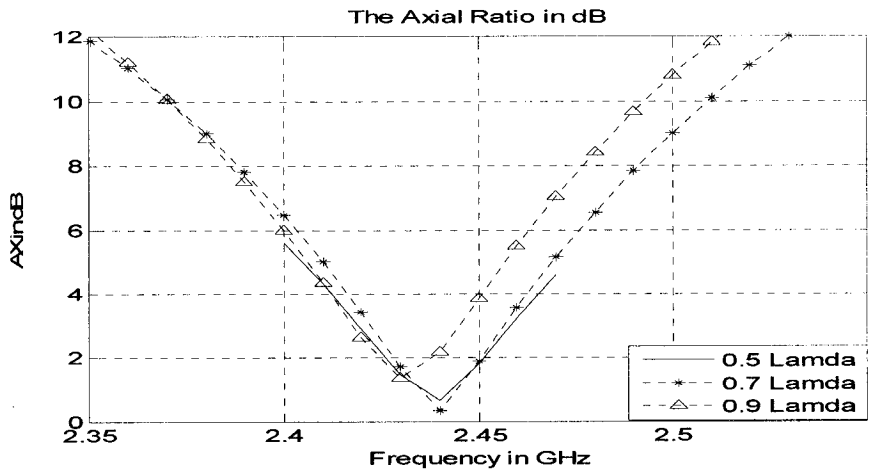

Figure 4.4: Axial ratios for the antenna array as a function of the distance between elements

4.4 Sequential Rotated Array Antennas

A wide band axial ratio antenna can be designed using a technique "Sequential Rotated Array," [42]. This orientation of an array is suitable for many types of antennas such as microstrip patches, horn, dipole, waveguide antennas. In this technique the antenna array consist of 2 elements or four or multiple of two that Arranged with an element angular orientation and the phase feeding between the elements is 0^0,90^0,0^0,90^0 or 90^0,0^0,180^0,270^0 ways as shown in figure 4.5. Sequential Rotated array has been investigated by many researches. In [43], it is concluded that the mutual coupling has miner affect on the antenna performance due to the orthogonal orientation of neighboring elements. The main beam of a sequential rotated array can be scanned from the main direction to a wide angle without serious deficiency on a performance of circular polarization.

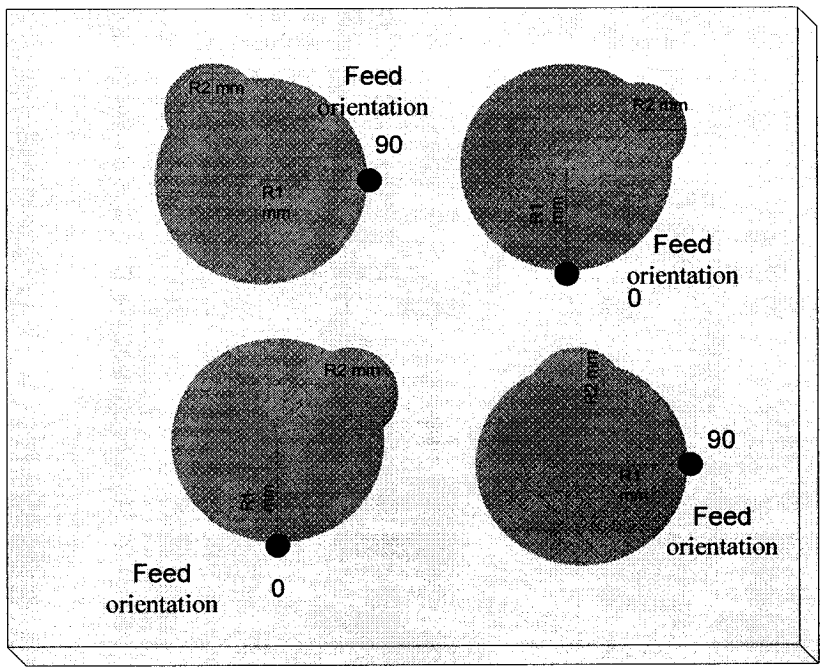

Figure 4.5: Four elements array design for a wide band axial ratio

The total radiated field by two elements arranged as a sequential rotated array antenna as shown in figure 4.6 is:

$$F_{xz} = H_1 e^{-jkd\sin\theta} e^{j0} + V_2 e^{jkd\sin\theta} e^{j90} + H_3 e^{jkd\sin\theta} e^{j0} + V_4 e^{-jkd\sin\theta} e^{j90} \qquad (4.1)$$

$$= \left(H_1 e^{j0} + V_4 e^{j90}\right) e^{-jkd\sin\theta} + \left(H_3 e^{j0} + V_2 e^{j90}\right) e^{jkd\sin\theta} \qquad (4.2)$$

F_{xz} is the field in the x - z plane, H_1 is the horizontal field from patch 1, and H_3 from the patch 2.

V_2 is the vertical field from the patch 2, and V_4 from the patch 2.

But

$H_1 = H_3$ and $V_2 = V_4$ which lead to:

$$F_{xz} = \left(He^{0} + Ve^{j90}\right)\left(e^{-jkd\sin\theta} + e^{jkd\sin\theta}\right) \quad (4.3)$$

$$F_{xz} = \left(He^{0} + Ve^{j90}\right)2.\cos(kd\sin\theta) \quad (4.4)$$

The two terms in the first bracket together represent a pure circularly polarized wave, and the cosine term is a two element array factor.

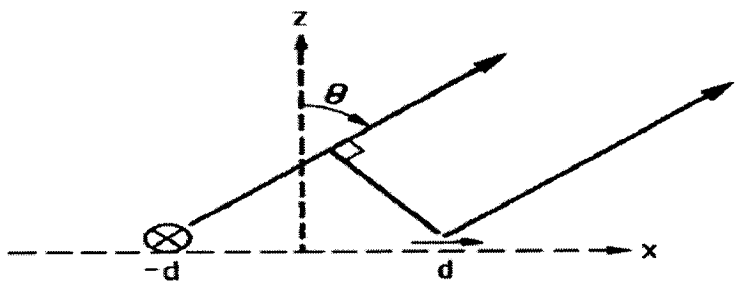

Figure 4.6: Two elements array for a wideband axial ratio [43]

4.4.1 Antenna Geometry

The phase rotation used in this design is $0^0, 90^0, 180^0, 270^0$. The phase delay in each patch is generated by changing the line length of the feed lines. The input impedance of the single patch is 200Ω. The input impedance of the single patch can be controlled with the orientation of the additional patch with respect to the orientation of the main patch. It is connected with 100Ω, which is connected with 50Ω at the end, as shown in figure 4.7. The distance between elements is $d_x = d_y = 47.2mm$.

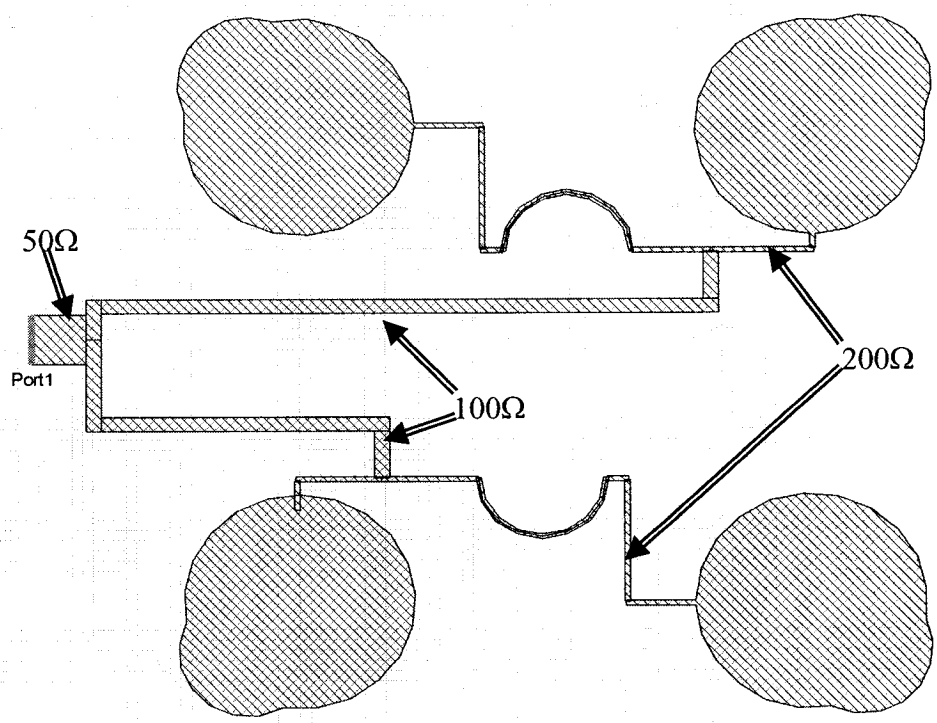

Figure 4.7: Four patches array, left hand circular polarization for a wide band axial ratio antenna

4.4.2 Simulated Results of the Antenna Array

Figure 4.8 demonstrates the radiation pattern (E_θ, E_ϕ) of the array antenna, which shows good circular polarization. Also, figure 4.9 shows the co-polarization and corss-polarization of the antenna array and it shows the LHCP is the dominant polarization. Figure 4.10 demonstrates a comparison between the axial ratio of the single patch antenna, and the four elements sequential rotted array antenna. The axial ratio bandwidth increased from 3.5% to 8.8 % with a better quality. Figure 4.11 presents the S_{11} results of the single antenna and the four elements antenna array that shows improvement of the input impedance bandwidth.

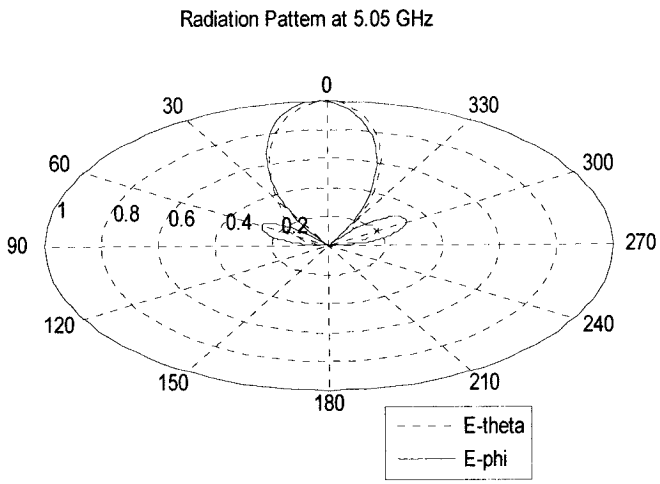

a

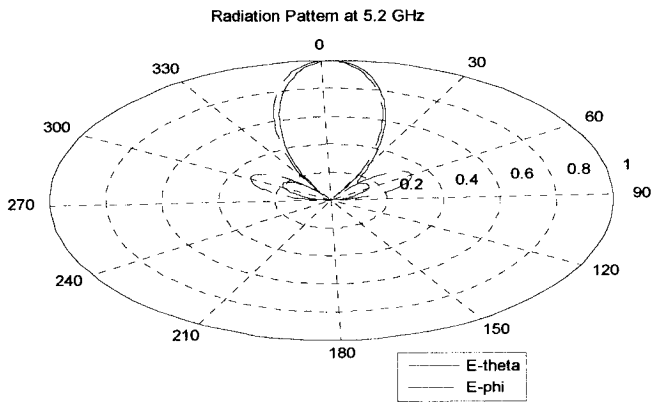

b

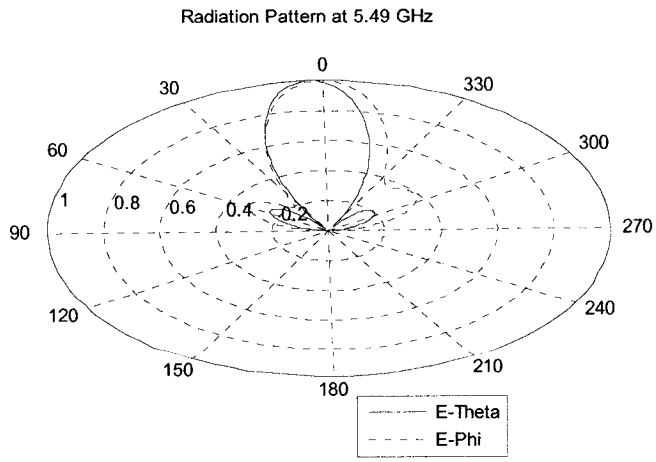

Figure 4.8: Radiation patterns of the antenna array
a) 5.05 GHz, b) 5.2GHz, c) 5.49GHz

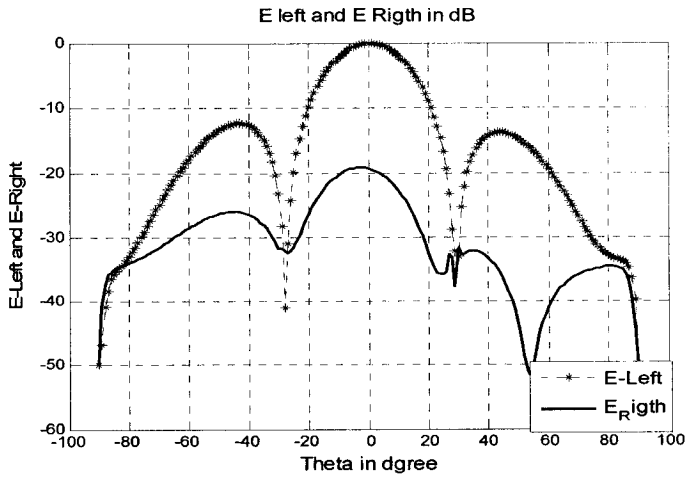

Figure 4.9: Co-polarization, and corss-polarization of the antenna array

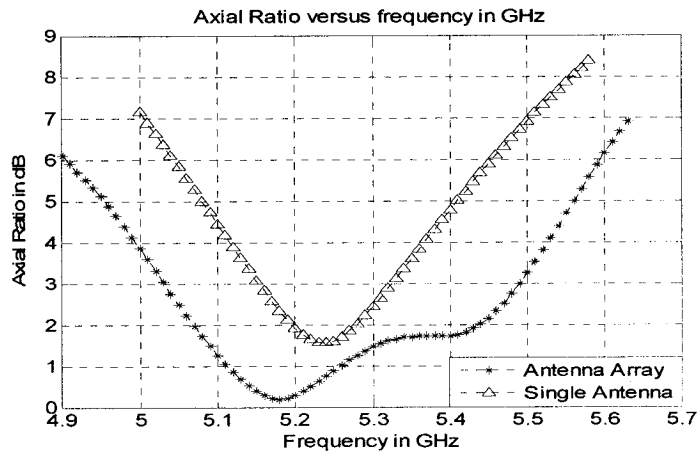

Figure 4.10: Axial ratio of the single element and the four elements patch antenna

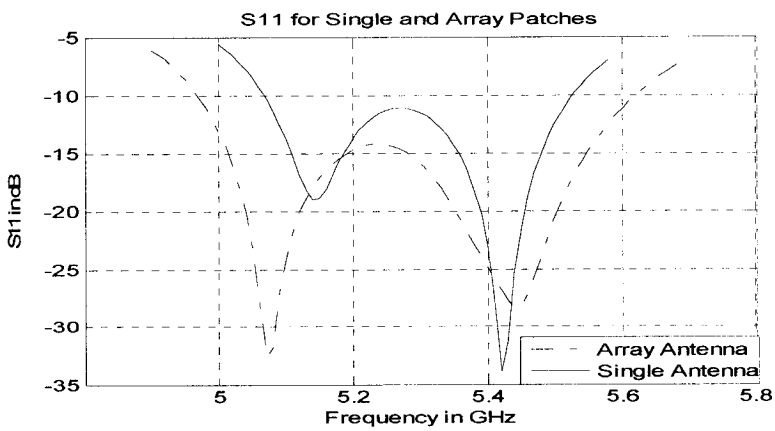

Figure 4.11: S11 of the single element and the four elements patch antenna

C h a p t e r F i v e

Conclusion and Future Work

5.1 Conclusion

In this thesis, single feed RHCP, LHCP, and Dual band antennas are designed for ISM wireless communication applications. A uniform linear array antenna for high directivity and a sequential antenna array for a wide band axial ratio are presented.

A novel design that uses an additional patch to create circular polarization is presented. Theoretical and experimental results are compared in order to demonstrate its ability as an alternative technique to generate a single feed circularly polarized antenna.

A novel design of a microstrip patch antenna consists of two circular patches fed with a coaxial cable has been implemented. The antenna covers both bands 2.45GHz, and 5.2 GHz. The theoretical and experimental results for return-loss impedance bandwidths show that the antenna bandwidth is 3.75% greater than a conventional circular microstrip patch antenna. The characteristics of the designed antenna depend strongly upon the position of the small additional patch and radii of the main and additional patch.

For other desired frequencies, the design of the antenna can be carried out by calculating the radii of the main and additional patch using empirical equations acquired for this design. The empirical formulas are developed based on a comprehensive parametric study where different designs and design parameters are varied to achieve an optimum antenna performance.

Another antenna design for circular polarization utilizing one microstrip feed line suitable for an integrated circuits demand is also investigated. Results demonstrate that both sense of circular polarization (RHCP, LHCP) can be achieved using this technique. A comparison between theoretical and experimental results is provided and it shows a good match. Different antenna parameters are investigated and showed good results as an alternative single feed circularly polarized antenna.

A 64-elements uniform linear array of circular microstrip patches is designed and simulated for achieving circular polarization with more than 20 dB directivity. A sequential rotated array is designed for a wide band axial ratio. A comparison between a single patch of the designed antenna with a four patches sequential rotated array with orientation of 0^0,90^0,0^0,90^0 shows that the axial ratio of the antenna array and the input impedance bandwidth improved to 8.8 % and 12.5 %, respectively. Also, the results of the antenna array show a good isolation between co-polarization, and cross-polarization.

5.2 Future Work

Further research may focus on study of dielectric covers effects on the performance of implemented antennas. The effects of a finite ground plane on the implemented antenna performance are another interesting topic for future research.

Appendix A

Cavity Model Technique for Circular Patch

A.1 Fields and Currents

The electric field in the cavity must satisfy a wave equation and the magnetic wall boundary condition. The solution of the wave equation in cylindrical coordinates is:

$$E_z = E_0 j_n(k\rho)\cos n\phi \quad \text{---------- (A.1)}$$

Where, $j_n(k\rho)$, is the Bessel functions.

The magnetic field components are:

$$H_\rho = \frac{j}{w\mu\rho}\frac{\partial E_z}{\partial \phi} = -\frac{jn}{w\mu\rho}E_0 j_n(k\rho)\sin n\phi \quad \text{---------- (A.2)}$$

$$H_\phi = -\frac{j}{w\mu}\frac{\partial E_z}{\partial \rho} = -\frac{jk}{w\mu}E_0 \bar{j}_n(k\rho)\cos n\phi \quad \text{---------- (A.3)}$$

The other field components are zero inside the cavity

$$E_\rho = E_\phi = H_Z = 0 \quad \text{---------- (A.4)}$$

The currents on the inner surface of the circular disk can be calculated from

$$\bar{J} = -\hat{Z} X \bar{H} = \hat{\rho} H_\phi - \bar{\phi} H_\rho \quad \text{---------- (A.5)}$$

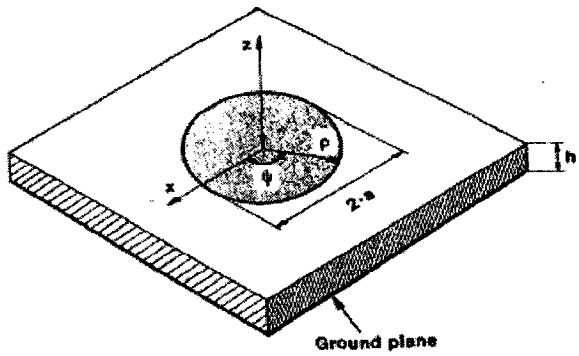

Figure A.1: circular microstrip disk antenna element [44]

A.2 Resonant Frequency

The resonant frequencies of the TM modes in the circular patch are given as [44-46]

$$f_{nm} = \frac{\alpha_{nm}.c}{2.\pi.a_{eff}.\sqrt{\varepsilon_r}} \quad \text{---------- (A.6)}$$

Where α_{nm} is the mth zero of the derivative of the Bessel function of order n, c is the velocity of light in free space, and ε_r is the relative dielectric constant of the substrate. The dominant mode is the TM_{11}.

For TM_{11} it has been recommended that [44]-[46],

$$a_{eff} = a.\left[1+\frac{2.h}{\pi.a.\varepsilon_r}\left(\ln\frac{.a}{2.h}\right)+(1.41\varepsilon_r+1.77)+\frac{h}{a}(0.268\varepsilon_r+1.6)\right]^{1/2} \quad \text{----- (A.7)}$$

A.3 Radiated Power

The power radiated through the upper half space is found by integrating the real part of the pointing vector over a closed surface [44].

$$P_r = \frac{1}{2\eta_0}\int_0^{2\pi}\int_0^{\pi/2}\left(|E_\theta|^2+|E_\phi|^2\right)r^2\sin\theta d\theta d\phi \quad \text{---------- (A.8)}$$

The numerical integration P_r estimated as:

$$P_r = \frac{(E_0 h)^2 \pi^3 a^2}{2\lambda_0{}^2 \eta_0}\left[\frac{4}{3} - \frac{8}{15}(k_0 a)^2 + \frac{11}{105}(k_0 a)^4 + ...\right] \text{ ---------- (A.9)}$$

The resonant radiation conductance G_r for a disk fed at an edge can be determined from the power radiated P_r as [44]:

$$P_r = \frac{1}{2} G_r (E_0 h)^2 = \frac{1}{2} G_r V_0{}^2 \text{ ---------- (A.10)}$$

$$R_r = \frac{1}{G_r} \text{ ---------- (A.11)}$$

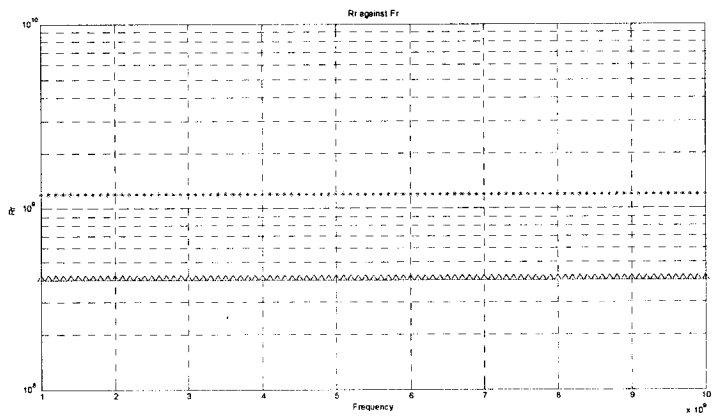

Figure A.2: R_r against Fr with dielectric constant 9.8 ****, and 2.2 ^^^^^^^^

Figure (A.2), shows the radiation resistance vary the frequency, which explain that high dielectric constant effect the radiated power that recommended for a patch antenna low dielectric constant, and for transmission lines high dielectric constant is recommended.

A.4 Directivity

The directivity of an antenna is defined as the ratio of the maximum power density to the average radiated power density [44].

$$D = \frac{(k.a)^2}{120.G_{rad}} \text{ ---------- (A.12)}$$

Where G_{rad} radiation conductance:

$$G_{ras} = \frac{(k.a)^2}{480}.\int_0^{\pi}\left[B_M{}^2(k.a.\sin\theta) + \cos^2\theta.B_p{}^2(k.a.\sin\theta)\right]\sin\theta.d\theta \text{ ---------- (A.13)}$$

The gain G of the antenna is defined as:

$$G = e_r D \text{ ---------- (A.14)}$$

Where e_r is the radiation efficiency of the antenna and it is in the range $0 < e_r < 1$.

A.4 Dielectric Losses

The power losses in the dielectric due to an imperfect substrate can be obtained by [44]:

$$G_{diel} = \frac{\varepsilon_{n0}.\tan\sigma}{4.\mu_0.h.f_{nm}}.\left[(k.a)^2 - n^2\right] \text{ ---------- (A.15)}$$

A.7 Input Impedance

The input impedance of the microstrip antenna is given by [44]:

$$Z_{in}(\rho) = \frac{1}{G}.\frac{j_n{}^2(k.\rho)}{j_n{}^2(k.a)} \text{ ---------- (A.16)}$$

The total conductance G is the sum of the equivalent conductance due to radiation, dielectric, and Ohmic losses.

A.8 Efficiency and Quality Factor

The radiation efficiency of the microstrip antenna is defined as the ratio of the radiated power to the input power [1]:

$$e_r = \frac{P_r}{P_i} = \frac{P_r}{P_r + P_c + P_d + P_{sur}} \quad \text{---------- (A.17)}$$

Where P_d is the power lost due to lossy dielectric of the substrate, P_c is the power lost due to finite conductivity of metallization, P_r is the power radiated in the free space wave, P_{sur} the power lost due to surface wave.

Also, the efficiency can be defined in terms of conductance as:

$$e_r = \frac{G_r}{G_r + G_{sur}} \quad \text{---------- (A.18)}$$

- *Quality Factor*

The total quality factor can be defined as [1]:

$$\frac{1}{Q} = \frac{1}{Q_d} + \frac{1}{Q_c} + \frac{1}{Q_r} + \frac{1}{Q_{sur}} \quad \text{---------- (A.19)}$$

Also, it is defined as the ratio between the energy stored in the system and the energy lost

$$Q = \frac{w_r W_T}{powerlost} \quad \text{---------- (A.20)}$$

$$\frac{1}{Q} = \frac{P_d + P_c + P_r + P_{sur}}{W_T w_r} \quad \text{---------- (A.21)}$$

The substrate material can be chosen such that at the desired resonant frequency $P_r \rangle P_c \rangle P_d$ fro a reasonably good radiation efficiency [44].

$$Q_d = \frac{1}{\tan\delta}$$ Loss tangent of substrate material ---------- (A.22)

$$Q_c = h\sqrt{\pi f \mu_0 \delta}$$ Conductivity of patch metallization ---------- (A.23)

$$Q_r = \frac{w_r W_T}{P_r}$$ ---------- (A.24)

$$W_T = \frac{hE_0^{\,2}}{8wf\mu_0} j_n^{\,2}(ka)\left((ka)^2 - n^2\right)$$ ---------- (A.25)

The Q factor has been calculated and plotted in [1]. Large bandwidth is possible by choosing a thicker substrate of a lower dielectric constant material.

References

[1] G. Ramesh "Microstrip Antenna Design Handbook", Artech House, 2001, ISBN 0-89006-513-6.

[2] R. Bancroft "Microstrip and Printed Antenna Design", Noble, 2004, ISBN 1-884932-58-4.

[3] J. Q. Howell "Microstrip Antenna," IEEE AP-S Int., Digest, pp. 177-180, 1972.

[4] M. Niroojazi "Practical Design of Single Feed Truncated Corner Microstrip Antenna," IEEE, Proceedings of the Second Annual conference on Communication Networks and Services Research, Fredericton, Canada, pp.301-304, May 2004.

[5] R. Ramire "Single- Feed Circularly Polarized Microstrip Ring Antenna and Arrays," IEEE Transaction Antenna and propagation, Vol.48, No.7, pp. 1040-104, July 2000.

[6] E. Fred "Broadband Patch Antennas," 1995 Artech House, Boston. London, ISBN 0-89006-777-5.

[7] J. Huang "Circularly Polarized Conical Patterns from Circular Microstrip Antennas," IEEE Transaction on Antenna and Propagation, Vol. AP-32, No. 9, pp.991-994 September 1984.

[8] A. E. Abdulhadi, and A.R Sebak. "Novel Design of Single Feed Right hand Circular Polarization with dual band," 12th International Symposium on Antenna Technology and Applied Electromagnetic [ANTEM] and Canadian radio sciences [URSI/CNC], July 2006.

[9] K. L. Wong "Compact and Broadband Microstrip Antenna," Wiley Inter Science, 2002, ISBN 0-471-41717-3.

[10] Y.T Lo, and W.F. Richard "Perturbation Approach to Design of Circularly polarized Microstrip Antennas," Electronics Letters, pp.383-385, May 1981.

[11] Y. J. Guo, and S. K. Batron "study on Ellipticity Properties of Single-Feed-Type Circularly Polarized Microstrip Antennas," Electronics Letters Vol. 18 No. 5, March 1982.

[12] K.L. Wong, W.H. Hsu, and C.K. Wu "Single-feed Circular Polarized Microstrip Antenna with A slit," Microwave and Optical Technology Letters Vol. 18, No. 4, pp.306-308, July 1998.

[13] K.P. Yang, K.L. Wong, and J.H. Lu "Single-Feed Slotted Equilateral-Triangular Microstrip Antenna for Circular Polarization," IEEE Transaction Antenna and propagation Vol. 47, No. 7, pp.1174-1178, July 1999.

[14] K.P. Yang, K.L. Wong, and J.H. Lu "Compact Circularly-Polarized Equilateral-Triangular Microstrip Antenna with Y-Shaped Slot," Microwave and Optical Technology Letters. Vol. 20, No.1, pp.31-34, January 1999.

[15] K. L. Wong, and Y. W. Jian "Single-Feed Small Circularly Polarized Square Microstrip Antenna," Electronics Letters Vol. 33 No. 22, pp. 1833-1834, October 1997.

[16] J. H. Lu, C. L. Tang, and K. L. Wong "Circular Polarization Design of a Single-feed Equilateral-Triangular Microstrip Antenna ," Electronics Letters 34, No. 4, pp. 319-321, February 1998.

[17] K. L. Wong, and M. H. Chen "Single –Feed Small Circular Microstrip Antenna with Circular Polarization," Microwave and Optical Technology Letters Vol.18, No.6, pp.394-397, August1998.

[18] H. M. Chen, and K.L. Wong "On the Circular Polarization Operation of Annular-Ring Microstrip Antennas," IEEE Transaction Antenna and propagation, Vol. 47, No. 8, pp. 1289-1292, August 1999.

[19] K. L. Wong, and Y. L. "Circularly Polarized Microstrip Antenna with a Tuning Stub," Electronics Letters Vol. 34, No. 9, pp. 831-832, April 1998.

[20] K.L. Wong, and M.H. Chen "Slot-Coupled Small Circularly Polarized Microstrip Antenna with Modified Cross-Slot and Bent Tuning-Stub," Electronic Letters Vol. 34, No. 16 pp. 1542-1543, August 1998.

[21] S. Maci, and G. Biff "Dual-Frequency Patch Antennas," IEEE Antenna and propagation, Magazine Vol. 39, No. 6, pp.13-21, December 1997.

[22] J. S. Chen, and K. L. Wong "A single-Layer Dual-Frequency Rectangular Microstrip patch Antenna Using a Single Probe Feed," Microwave and Optical Technology Letters , Vol. 11, No. 2, PP. 83-84, 1996.

[23] S. A. long, and M. D. Walt "A Dual-Frequency Stacked Circular –Disc Antenna," IEEE Transaction and Antenna propagation Vol.27, No.3, PP. 1281-1285, March 1979.

[24] D. M. Syankal, and H. R. Hassani "Characteristics of Stacked Rectangular and Triangular Patch Antennas for Dual Band Application," IEE 8th International Conference on Antennas and Propagation, Edinburgh, pp. 196-199, March 1993.

[25] C. Salvador, L. Borselli, A. Falciani, and S. Maci, "A Dual Frequency Planar Antenna at S and X Bands," Electronics Letters Vol. 31, No. 20, PP. 1706-1707, October 1995.

[26] K. L. Wong, and W. S. Chen "Compact Microstrip Antenna with Dual-Frequency Operation," Electronic Letters Vol. 33, No. 8, pp. 646-647, April 1997.

[27] C. L. Tang, H. T. Chen, and K. L. Wong "Small Circular Microstrip Antenna with Dual-Frequency Operation," Electronics Letters Vol. 33, No.13, pp.1112-1113, June 1997.

[28] S. C. Pan, and K. L. Wong "Dual-frequency Triangular Microstrip Antenna with a Shorting Pin," IEEE Transaction Antenna and Propagation Vol. 45, No. 12. pp. 1889-1891, December 1997.

[29] J. H. Wang "Generalized Moment Methods in Electromagnetic," John Wiley & Sons, Inc, 1991, ISBN 0-471-51443-8.

[30] P.N. Commander, and C. D. Dombowsky "Circularly Polarized Rectangular Dialectic Resonator Antenna for Personal Communications," MSc. Thesis Department of Electrical and Computer Engineering, Royal Military College of Canada, 1996.

[31] J. R. Mosig, and F. E. Gardiol, "General Integral Equation Formulation for Microstrip Antennas and Scatters," IEE Proc. Microwave and Optical Technology Letters, Vol. 132, pp. 424-432, December 1985.

[32] S. Raut "An efficient Method for the Design and Analysis of Microstrip Circuits and Antennas," M.Sc. Thesis Department of Electrical and Computer Engineering, University of Manitoba, Canada, 1997.

[33] J. Moore, and R. Pizer "Moment Methods in Electromagnetic," John Wiley & Sons, Inc, 1984, ISBN 0-471-904147.

[34] D. G. Swanson "Microwave Circuit Modeling Using Electromagnetic Field Simulation," Artech house, 2003, ISBN 1-58053-308-6.

[35] D. M. Pozar "Input Impedance and Mutual Coupling of Rectangular Microstrip Antennas," IEEE Transaction Antenna and Propagation, Vol. 30, No.6, pp. 740-747, November 1985.

[36] H. Edward, and P. Tulyathan "Analysis of Microstrip Antennas Using Moment Method," IEEE Transaction Antenna and Propagation, Vol. 29, No.1, pp. 47-76, January 1981.

[37] M. D. Deshpande "Analysis of Slot Loaded Microstrip Antenna Using Moment Method," IEEE Transaction Antenna and Propagation, Vol.11, No.5 pp. 467-470, 1989.

[38] M. C. Bailey, and M. D. Deshpande "The Moment Method Solution for Printed Wire Antennas of Arbitrary Configuration," IEEE Transaction Antenna and Propagation, Vol. 36, No. 12, pp. 1667-1676, December 1988.

[39] M. C. Bailey, and M. D. Deshpande "Analysis of Elliptical and Circular Microstrip Antennas Using Moment Method," IEEE Transaction Antenna and Propagation, Vol.33, No. 9, pp. 954-959, September 1985.

[40] J. P. Damiano, and A. Papiernik " Survey of Analytical and Numerical Models for Probe-Fed Microstrip Antennas," IEE Proc. Microwave Antennas and Propagation, Vol. 141, No. 1, pp. 15-22, February 1994.

[41] A. E. Abdulhadi, and A. R. Sebak "Single Feed Circularly Polarized Microstrip Antenna Array,"2nd International ITG Conference on Antennas, Arabella Sheraton, Munich , March 2007.

[42] A. E. Abdulhadi, and A. R. Sebak, "Single Feed Circular Polarized Antenna and Array," IEEE AP-S International Symposium, Honolulu, Hawaii USA, June 2007.

[43] J. Huang "A Technique for an Array to Generate Circular Polarization with Linearly Polarized Elements," IEEE Transactions Antenna and propagation, Vol. 34, NO. 9, pp. 601-607, September 1986.

[44] A. G. Derneryd "Analysis of the Microstrip Disk Antenna Element," IEEE Transaction Antenna and propagation, Vol. 27, No. 5, pp 660-664, September 1979.

[45] C. Shen, S. A. Long, M. R. Allerding, and M. D. Walton "Resonant Frequency of a Circular Disc Printed-Circuit Antenna," IEEE Transaction Antenna and propagation, Vol. 25, No. 4, pp. 445-449, July 1977.

[46] J. Watking "Circular Resonant Structures in Microstrip," Electronics Letters, Vol. 5, No. 21, pp. 524-525, October 1969.